# Supplementary Information

Anthropogenic signature of global agricultural soil phosphorus

## Table of Contents


Table of Contents ..... 1

1. Countries considered ..... 2

2. Calculation of Input data ..... 2

2.1 Manure (OF) ..... 2

2.2 P harvest from agricultural areas ..... 3

2.2.1 P harvest from grasslands ..... 4

2.2.2 P harvest from croplands ..... 5

2.3 Losses (LO) ..... 5

2.4 Use of mineral P fertilizer (CF) ..... 6

2.5 Use of mineral feed (MF) ..... 6

2.6 Sludge (SL) ..... 7

2.7 Labile P pool available data ..... 7

2.7.1. From another global modelling approach: Ringeval et al. 2017 ..... 7

2.7.2. From field measurements ..... 8

3 Calculation of the anthropogenic signatures of P fluxes and pools ..... 9

3.1 General definition ..... 9

3.2 Anthropogenic signature of manure ..... 10

3.3 Anthropogenic signature of sewage sludge ..... 11

4 Calculation of Imported Feed and Food quantities ..... 12

4.1. Imported Feed ..... 12

4.2. Imported Food ..... 14

5 Land expansion/abandonment ..... 14

6 Calibration: methodology and results ..... 14

6.1. Methodology of the calibration procedure ..... 14

6.2. Results from the main calibration procedure ..... 16

6.3. Result of the second calibration - with observed data used to constraint the size of the labile P pool ..... 17

7 Data analysis ..... 18

8 Main drivers of the values and temporal evolutions of the soil P anthropogenic signatures ..... 19

8.1 Drivers of the anthropogenic signatures of the total soil P pools ..... 19

8.2 Drivers of the anthropogenic signatures of the soil labile P pool ..... 20

9 Estimates of the size of the soil labile and stable P pools ..... 21
Supplementary Figures ..... 22
Supplementary Tables ..... 41
References ..... 47

# 1. Countries considered

In this work, we considered 132 countries. Their repartition between the seven main regions studied is given in Figure S1.

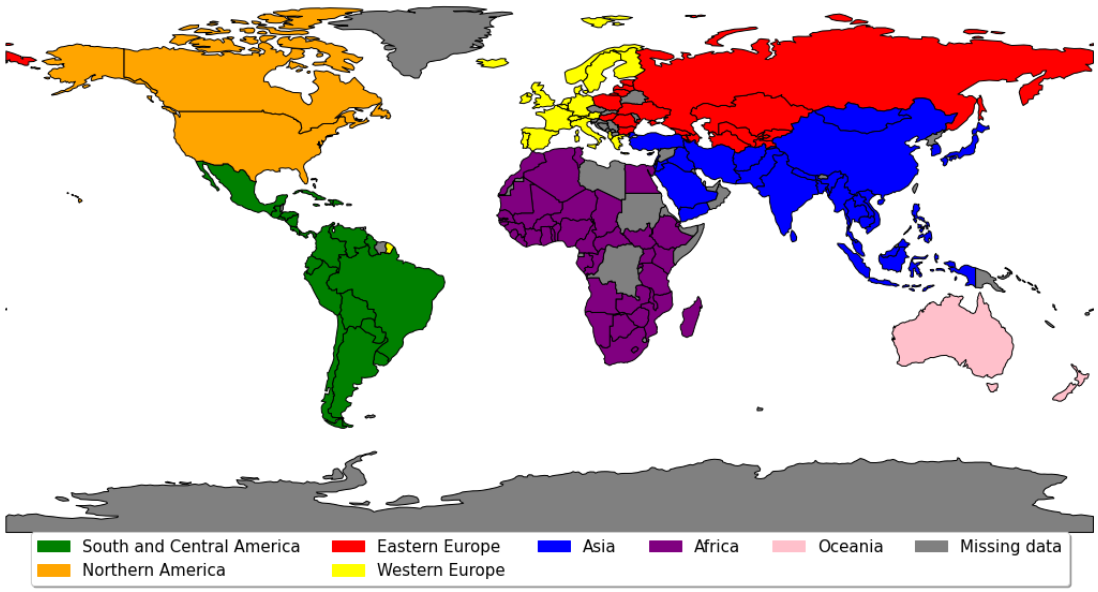


*Figure S1 – Repartition of the countries considered between the different world regions.*

Some countries were excluded because we lack data regarding some of the inputs required to run the calculations. For example, we missed data on the trade of agricultural products for Democratic Republic of Congo, Libya and Somalia. Besides, some countries were not analysed in our results as our calibration did not work for these countries (see Section **S6**).

# 2. Calculation of Input data

## 2.1 Manure (OF)

For each year, for each country, the annual inputs of P under the form of manure to agricultural soils (both croplands and grasslands) were calculated with Equation **S1**.

*Equation S1 – Soil P inputs as manure*

$$OF_{Tot}(y,c) = \frac{1}{A(y,c)} \sum_{l=1}^{8} Heads(l,c,y).P_{excretion}(l,c,y)$$

$OF_{Tot}(y,c)$ is in kgP.ha$^{-1}$. $A(y,c)$ refers to the total cropland and grassland areas of the country *c* at year *y* (in ha). The data used are derived from HYDE 3.2 (Klein Goldewijk et al., 2017). $Heads(l,c,y)$ refers to the number of heads of the animal category *l* for country *c* at year *y*. We considered 8 animal categories including Asses&Mules, Cattle, Poultry, Goats&Sheep, Horses, Buffaloes, Pigs and Rabbits&hares (see Table **S2**). For the 1961-2017 period, we used the data from FAOSTAT. For the 1950-1960 period, we retrieved data from the International Historical Statistics (Mitchell, 1998b, 1998a, 1993). Often data were missing for some years. When possible a linear interpolation was performed to fill the missing data based on the two closest values. When no data was available, either for the country or for one of the animal category considered, the number of heads was calculated based on the number of heads in 1961 and the human population at year *y* and at year 1961, assuming a proportional relationship between these two variables (human and animal population). $P_{excretion}(l,c,y)$ corresponds to the P excretion rate of the animal category *l* for the country *c* at year *y*. It is in kgP.head$^{-1}$.yr$^{-1}$. It was calculated with Equation **S2**.

*Equation S2 – P excretion rates*

$$P_{excretion}(l,c,y) = P_{rate}(l).SW(l,c,y)$$

Where $P_{rate}(l)$ refers to the P excretion rate per kg of slaughtered weight for the livestock category *l* (see Table **S3**). $SW(l,c,y)$ refers to the slaughtered weight of livestock category $l$ in the country *c*, at year *y*. When possible we used the slaughtered weight data from FAOSTAT (in FAOSTAT referred to as carcass weight). When information on slaughtered weight was not available (mostly for mules and asses), we used regional average. For the 1950-1960 period, we assumed that the slaughtered weights were the same as those in 1961. Raw and final data can be found in the attached repository (see **Code and data availability**).

## 2.2 P harvest from agricultural areas

To perform the calibration of the model parameters, we calculated the total annual P harvest from both cropland and grasslands for each country, using Equation **S3**.

*Equation S3 – P harvest from both croplands and grasslands*

$$P_{harvest,Tot}(c,y) = \frac{1}{A(c,y)}.\left(Forage_{P_{harvest}}(c,y) + Crop_{P_{harvest}}(c,y)\right)$$

Where $P_{harvest,Tot}(c,y)$ was in kgP.ha$^{-1}$. $Forage_{P_{harvest}}(c,y)$ and $Crop_{P_{harvest}}(c,y)$ refer to the P harvest from grasslands and croplands, respectively. They are expressed in kgP. The subscript "Tot" refers to the sum of both anthropogenic (Ant) and natural (Nat) P.

### 2.2.1 P harvest from grasslands

P harvest from grasslands was assumed to be equal to the forage domestic P demand (in kgP) and was calculated with Equation **S4**.

*Equation S4 – Forage P harvest*

$$Forage_{P_{harvest}}(c,y) = \sum_{l=1}^{6} Req(l).LW(l,c,y).Heads(l,c,y).Share_{feedASforage}(l,c).E_c.concP$$

Where the livestock categories considered were dairy cattle, beef, sheep for meat, sheep for milk, goat for meat and goat for milk. $E_c$ corresponds to the energy content of 1 kg of dry forage. A value of 10 MJ.kg DM$^{-1}$ was used. $concP$ is the P content of forage. We assumed a value of 0.003 tP.tDM$^{-1}$ (Comifer, 2009). $LW(l,c,y)$, expressed in kg per head, refers to the live weight of the animal category *l* in the country *c*, at year *y*. It was calculated as shown in Equation **S5**.

*Equation S5 – Live weights*

$$LW(l,c,y) = SW(l,c,y).ratio(l)$$

In which, $SW(l,c,y)$ refers to a slaughtered weight in kg.head$^{-1}$ and the $ratio(l)$ refers to a coefficient that enables the conversion from slaughtered to live weight. We assumed a ratio of 0.548 for cattle dairy and beef and of 0.5 for all goats and sheep.

The $Share_{feedASforage}(l,c)$ is the fraction of the total energy that the livestock category *l* consumes as forage and occasional fodder. It was calculated based on Equation **S6** and the data from (Herrero et al., 2013). The $Share_{feedASforage}(l,c)$ was the same for countries belonging to the same world region (*r*) as defined in (Herrero et al., 2013). In Equation **S6** we calculated weighted regional average of the fraction of forage and occasional fodders of livestock feed intake. The weight was performed based on the number of productive animals in each livestock production system (*LPS*).

*Equation S6 – Share of the forage and occasional fodder in the total feed consumed*

$$Share_{feedASforage}(l,c) = \frac{\sum_{LPS} Number_{productive}(LPS,r,l).Perc_{grass}(LPS,r,l)}{\sum_{LPS} Number_{productive}(LPS,r,l)}$$

$LPS$ and *r* refer respectively to livestock production system and world regions as described in (Herrero et al., 2013). $Number_{productive}(LPS, r, l)$ refers to the number of productive heads at year 2000 (Table S11 of Herrero et al. 2013). $Perc_{grass}(LPS, r, l)$ refers to the percentage of the feed intake consumed as grass and occasional fodders (Table S10 of Herrero et al. 2013).

$Req(l)$ is the energy requirement, expressed in MJ.yr$^{-1}$.kg of live weight$^{-1}$, of the livestock category *l*. Data were derived from (Barbieri et al., 2021) and are shown in Table **S4**.

Finally, the number of heads of each of the ruminant considered (referred to as $Heads(l, c, y)$ in Equation **S4**) was calculated by combining FAOSTAT data on livestock numbers (which do not distinguish meat vs milk), and milk and meat production for each specie.

### 2.2.2 P harvest from croplands

To compute P harvest from cropland for the 1961-2017 period, we used Production data provided by FAOSTAT. We considered 31 different items, as shown in Table **S5**. For each item, we multiplied the quantities produced (in tonnes) by their P content (see concP, Table **S5**). The obtained data were divided by the total agricultural areas to compute a flux in kgP.ha$^{-1}$.

For the 1950-1960 period, we derived the quantities produced from those produced in 1961 by assuming that these values where proportional to the human population, as shown in Equation **S7**.

*Equation S7 – P harvest from croplands for the period 1950-1960*

$$\forall y \in [1950 - 1960],\ \ Crop_{P_{harvest}}(c, y) = Crop_{P_{harvest}}(c, 1961).\frac{HumanPop(c, y)}{HumanPop(c, 1961)}$$

## 2.3 Losses (LO)

In our approach, we considered only the soil P losses due to soil erosion but neglected that caused by leaching. Our calculations followed the methodology used by (Ringeval et al., 2017) and is based on soil erosion data from (Van Oost et al., 2007). The latter computed global estimates of sediment mobilized by water erosion, with a cropland/grassland distinction. We assumed that these estimates (in kg of soil.ha$^{-1}$.yr$^{-1}$) provided for year ~2000 were representative of the whole study period. For each country, we first averaged the available data based on the relative proportion of croplands and grasslands at year 2000. This gave us an average soil erosion rate per agricultural area in kg of soil.ha$^{-1}$.yr$^{-1}$. This information was then divided by the soil stock in order to get a fraction of the soil that was lost per year. The soil stock was computed assuming a soil depth of 30 cm (see **Method** in the Main Text) and a soil bulk density of 1.4 g.cm$^{-3}$.

Eventually, P losses from all P pools were calculated annually based on the estimated fraction of soil lost (called *p*) and the size of each P pool - estimated through our approach- (Equation **S8**).

*Equation S8 – Soil P losses*

$$LO_{SP,X}(y,c) = SP_X(y,c).p(c)$$

$$LO_{LP,X}(y,c) = LP_X(y,c).p(c)$$

Where *X* stands for the sub-scripts *Nat* and *Ant*. *p* is the fraction of soil lost in country *c* for each year (no unit).

## 2.4 Use of mineral P fertilizer (CF)

For the 1961-2018 period, we retrieved data on the use mineral P fertilizer from FAOSTAT. We converted the tonnes of $P_2O_5$ to tonnes of P using a conversion factor of 0.44. The total quantities applied to agricultural soils were divided by the areas under grasslands and croplands to compute application rates in $kgP.ha^{-1}$.

For the 1950-1960 period, we used the spatially explicit data on the use of mineral P fertilizer per area of cropland ($gP.m^{-2}.yr^{-1}$) from (Lu and Tian, 2016), which we aggregated per country. The data were only available for the years 1950 and 1960. We thus performed a linear interpolation to fill the missing years.

## 2.5 Use of mineral feed (MF)

We assumed that 5% of the global annual $P_2O_5$ extracted quantities (derived from FAOSTAT) were used to produce mineral feed additives for livestock animals (Cordell and White, 2014; Smil, 2000). See Equation **S9**.

*Equation S9 – Annual consumption of mineral feed globally (kgP)*

$$MF_{Tot}(y) = 0.05 * 0.44 * GlobalUse_{P_2O_5}(y)$$

Where $MF_{Tot}(y)$ is the global use of mineral feed at year *y*. The $GlobalUse_{P_2O_5}(y)$ information, in kg $P_2O_5$ was directly derived from FAOSTAT International database.

Then we allocated $MF_{Tot}(y)$ to each country (see Equation **S10**) based on an allocation coefficient $f_{MF}(y,c)$, that we calculated with Equation **S11**.

*Equation S10 – Mineral feed annual consumption of each country*

$$MF(y,c) = MF_{Tot}(y).f_{MF}(y,c)$$

*Equation S11 – Allocation coefficient of the global annual consumption of mineral feed*

$$f_{MF}(y,c) = \frac{1}{2}.\left(f_{LU}(y,c) + f_{CF}(y,c)\right)$$

Equation **S11** is based on the assumption that the use of mineral feed in each country depends on their livestock density and on their use of mineral P fertilizer. $f_{LU}(y,c)$ refers for each country to the fraction of the global livestock they have (accounted for in livestock unit). Similarly, $f_{CF}(y,c)$ refers to the fraction of the global use of mineral P fertilizer a country consumed. We averaged both information to calculate an allocation coefficient for each country. When a country did not use any mineral P fertilizer, we set $f_{MF}(y,c)$ to zero. Data and calculation details can be found in the repository attached (see **Code and Data availability**).

## 2.6 Sludge (SL)

We calculated the flux of P contained in sewage sludge coming from the human food consumption, but excluded that coming from detergents as we lack data to properly estimate them. For each country *c*, for each year *y*, P in sludge was calculated with Equation **S12**. The methodology and the data used were derived from (Van Puijenbroek et al., 2019).

*Equation S12 – Soil P inputs as sludge*

$$SL_{Tot}(y,c) = \frac{1}{A(y,c)}.HumanPop(y,c).E_{hum}.\sum_{t=1}^{3} T(y,c,t).NR^{P}(t) \qquad \forall y \in \{1990,2000,2010\}$$

Where $SL_{Tot}(y,c)$ was the flux of P contained in sludge that was applied to agricultural soils in kgP.ha$^{-1}$.yr$^{-1}$. The subscript "Tot" refers to the sum of both anthropogenic (Ant) and natural (Nat) P. $A(y,c)$ was the total cropland and grassland area (in ha), $HumanPop(y,c)$ was the total human population in persons, $E_{hum}$ was the P excretion rate of humans in kgP.cap$^{-1}$.yr$^{-1}$, $T(y,c,t)$ was the percentage of the households of country *c* with waste water treatment primary (t=1), secondary (t=2) and tertiary (t=3) and $NR^{P}(t)$ was the P removal fraction for primary, secondary and tertiary waste water treatment. $E_{hum}$ was set to 0.5 kgP.cap$^{-1}$.yr$^{-1}$ independently of the country considered (Smil, 2000). For the missing years, we performed linear interpolations with the closest values. That flux reached up to 9.5 kgP.ha$^{-1}$.yr$^{-1}$ in the Republic of Korea in 2017 with an average global value of 0.1 kgP.ha$^{-1}$.yr$^{-1}$ in 2017.

## 2.7 Labile P pool available data

### 2.7.1. From another global modelling approach: Ringeval et al. 2017

For each country, the size of the labile pool that we used to constrain the model was derived from the results of (Ringeval et al., 2017).

Ringeval et al. simulated the evolution of the soil P content at the global scale from 1700 to 2005 with a yearly time step, using a six-pool model. Their approach was spatially explicit at half-degree resolution. They simulated separately the soil P evolution of croplands and of grasslands. Among soil P pools considered in Ringeval et al., the inorganic labile pool (so-called PILAB in the following) correspond to the sum of H2O Pi + Resin Pi + Bicarbonate Pi Hedley fractions. We assumed here that PILAB could be used to approach our labile pool.

Ringeval et al. provided a mean and standard deviation of PILAB at half degree resolution for both cropland and grassland. Here, for a given country, we computed the mean and standard deviation at country scale of PILAB for agricultural soils (cropland + grassland) as the average of the mean/std among all grid-cells within the country considered, with the average being weighted by the agricultural area of each grid-cell.

Only the value representative of the last year available in Ringeval et al. (Ringeval et al., 2017), i.e. 2005 were used for the calibration procedure.

### 2.7.2. From field measurements

When data were available we calibrated the model with real data on the P availability of agricultural soils (see Table **S6** for European countries and Figure **S2** for all countries). The challenge was to found enough data both on croplands and grasslands that would be representative of the "real" agricultural soils of each country. We were only able to collect data for some European countries, Canada, the USA, Tanzania, Yemen and Botswana. Soil depths considered in the different databases ranged from 20 to 40 cm. We always assumed to the available data were representative of the 0-30 cm soil horizon.

For European countries we derived the P-Olsen data from the LUCAS topsoil survey conducted in 2015 (Jones et al., 2020). As part of this survey, soil samples had been collected on croplands, grasslands, woodlands, shrublands, wetlands, barelands, and others. For the purpose of this work, we kept only the data from the land use 'Agriculture (excluding fallow land and kitchen gardens)'. For each country, the P-Olsen values above 10mgP/kg (detection limit) were averaged. The conversion from mgP/kg of soil to kgP.ha$^{-1}$ was done using a soil bulk density of 1.4 g.cm$^{-3}$ and a soil depth of 30 cm. Countries with less than 20 measurement points were excluded.

For the USA and Canada we retrieved data from the Fertilizer Institute – Soil Test Summary (Bray and Kurtz P1 equivalent) (IPNI, 2015). From the AfSIS (Africa Soil Information Service) Sentinel Sites we retrieved Mehlich-3 data for Tanzania (Hengl et al., 2017). Finally, for Yemen and Botswana, we found P-Olsen data in the ISRIC-WISE soil database (Batjes, 2010) – see **Code and Data availability** for more details.

We compared the obtained data with the outputs from (Ringeval et al., 2017) and got in some cases large differences (Figure **S2**). These could be explained by several reasons. First, chemical extractions could differ: Ringeval et al. modelling approach is based on Hedley fractionation method while country-scale dataset are based on Olsen-P (European countries, Yemen and Botswana), Mehlich-3 (Tanzania) or Bray and Kurtz P1 equivalent (USA and Canada). Second, for some countries, the number of sites considered and/or their spatial distribution within the country make their average not representative to country-scale agricultural soil P. Last, years represented by Ringeval et al. (year 2005) and of observed data (mainly 2015) do not match.

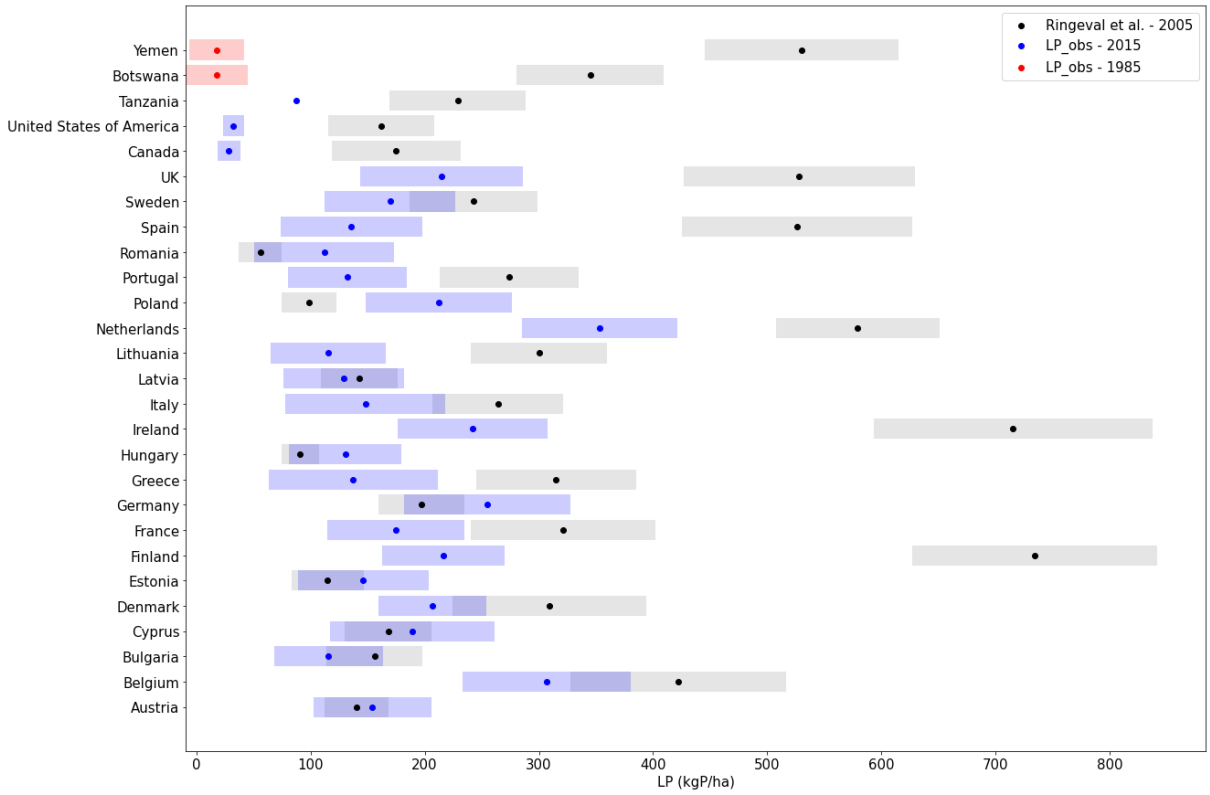


*Figure S2 – Comparison of agricultural soil available P data from Ringeval et al. 2017 (in dark) and from measurements we managed to collect. Data from Ringeval et al. 2017 refers to their PILAB data at year 2005. In blue are the P-Olsen data we collected for European countries (Jones et al., 2020), the Bray and Kurtz P1 equivalent data we collected for the USA and Canada (IPNI, 2015) and the Mehlich-3 data for Tanzania (Hengl et al., 2017). All refer to year 2015. In red are the P-Olsen data for Yemen and Botswana. They were likely collected around the year 1985 (Batjes, 2010). Dots and bars represent respectively the mean and standard deviation values in kgP.ha$^{-1}$*

# 3 Calculation of the anthropogenic signatures of P fluxes and pools

## 3.1 General definition

The anthropogenic signature of each P pool and P flux X was defined as the ratio of the anthropogenic component of that pool or flux over its total value, as shown in Equation **S13**.

*Equation S13 – Anthropogenic signature general definition*

$$SignAnt_X(y,c) = \frac{X_{Ant}(y,c)}{X_{Tot}(y,c)}$$

With Tot refers to the sum of anthropogenic (Ant) and natural (Nat, as used in the main text).

## 3.2 Anthropogenic signature of manure

The anthropogenic signature of manure was equal to the ratio of P in manure from anthropogenic origin divided by the total P in manure, as shown in Equation **S14**.

*Equation S14 – Anthropogenic signature of manure*

$$SignAnt_{OF}(y,c) = \frac{OF_{Ant}(y,c)}{OF_{Tot}(y,c)}$$

Where $OF_{Ant}(y,c)$ and $OF_{Tot}(y,c)$ are in kgP.ha$^{-1}$.yr$^{-1}$. The ratio was calculated annually for each country. $OF_{Ant}(y,c)$ was calculated with Equation **S15** and $OF_{Tot}(y,c)$ with Equation **S1**.

*Equation S15 – P in manure from anthropic origin*

$$OF_{Ant}(y,c) = OF_{Tot}(y,c).\frac{MF(y,c) + ImpFeed_{Ant}(y,c) + DosmesticFeed_{Ant}(y,c) + Forage_{Ant}(y,c)}{MF(y,c) + ImpFeed_{Tot}(y,c) + DosmesticFeed_{Tot}(y,c) + Forage_{P_{harvest}}(y,c)}$$

In the above Equation, the fraction that multiplies $OF_{Tot}(y,c)$ refers to the anthropogenic signature of the livestock feed intake. As a result, it is the ratio of livestock anthropogenic P feed and forage intake over total livestock P feed and forage intake. $Forage_{P_{harvest}}(y,c)$, in kgP.yr$^{-1}$, referred to the total forage demand as calculated with Equation **S4**. We assumed that all the forage consumed was domestically produced. As a result, the anthropogenic signature of that flux was equal to that of the labile P pool of the country considered (see Equation **S16**).

*Equation S16 – P in forage from anthropogenic origin*

$$Forage_{Ant}(y,c) = Forage_{P_{harvest}}(y,c).\frac{LP_{Ant}(y,c)}{LP_{Tot}(y,c)}$$

For each country, for each year, the total imported feed ($ImpFeed_{Tot}(y,c)$, kgP) and domestically produced feed ($DomesticFeed_{Tot}(y,c)$, kgP) were calculated with Equation **S17** and Equation **S18**, respectively.

*Equation S17 – Total imported feed*

$$ImpFeed_{Tot}(y,c) = \sum_{k=1}^{N}\sum_{i=1}^{55} ImpFeed(y,c,k,i)\,.\,concP(i)$$

*Equation S18 – Total domestically produced feed*

$$DomesticFeed_{Tot}(y,c) = \sum_{i=1}^{55} Feed(y,c,i).concP(i) - ImpFeed_{Tot}(y,c)$$

Where *k* referred to the partner countries that export their agricultural products to the country *c*, *N* referred to the total number of partner countries and *i* to the agricultural items. For this work we restricted the analysis to 55 items, which represented more than 85% of the total P traded as agricultural products at the global scale. All the items and their corresponding names in the FAOSTAT databases are provided in Table **S7**. $Feed(y,c,i)$ was in kgDM and referred to the total amount of feed consumed as item *i*. The sum of all these quantities multiplied by their P concentration gave the total feed consumption in the country *c*, at year *y*. By subtracting to it the total amount of feed imported (in kgP), we induced the quantities of feed that was domestically produced (in kgP, see Equation **S18**). From 1961, the feed consumption of each item $Feed(yr,c,i)$ was directly derived from the Food Balances database from FAOSTAT. For the 1950-1960 period, we estimated the feed consumed for each item based on the feed consumption in 1961 and the livestock density (referred to as $LU(y,c)$, in livestock unit) at year *y* and at year 1961, as shown in Equation **S19**.

*Equation S19 – Feed consumption for the period 1950-1960*

$$\forall y \in [1950-1960], \qquad Feed(y,c,i) = LU(y,c).\frac{Feed(1961,c,i)}{LU(1961,c)}$$

Finally, the amount of imported feed from anthropic origin $ImpFeed_{Ant}(yr,c)$, expressed in kgP was calculated with Equation **S20**.

*Equation S20 – Anthropogenic imported feed*

$$ImpFeed_{Ant}(y,c) = \sum_{k=1}^{N}\sum_{i=1}^{25} ImpFeed(y,c,k,i).concP(i).\frac{LP_{Ant}(y,k)}{LP_{Tot}(y,k)}$$

## 3.3 Anthropogenic signature of sewage sludge

The anthropogenic signature of sewage sludge was calculated as the ratio of anthropogenic P in sludge divided by the total P in sludge, as shown in Equation **S21**.

*Equation S21 – Anthropogenic signature of sludge*

$$SignAnt_{SL}(y,c) = \frac{SL_{Ant}(y,c)}{SL_{Tot}(y,c)}$$

Where $SL_{Ant}(y,c)$ and $SL_{Tot}(y,c)$ were expressed in kgP.ha$^{-1}$.y$^{-1}$. The ratio was calculated annually for each country. $SL_{Ant}(y,c)$ was calculated with Equation **S22** and $SL_{Tot}(y,c)$ with Equation **S12**.

*Equation S22 – Anthropogenic P in sludge*

$$SL_{Ant}(y,c) = SL_{Tot}(y,c).\frac{Food_{Ant}(y,c)}{Food_{Tot}(y,c)}$$

$Food_{Tot}(y,c)$ referred to the total food consumed (in kgP). $Food_{Ant}(y,c)$ referred to the total anthropogenic food consumed. Before 1961, we neglected imported food products. As a result, the anthropogenic food consumed was calculated as the total food consumed multiplied by the anthropogenic signature of the labile P pool. From 1961, $Food_{Ant}(y,c)$ was calculated with Equation **S23**.

*Equation S23 – Anthropogenic P in the food consumed*

$$Food_{Ant}(y,c) = SelfProducedFood(y,c)\frac{LP_{Ant}(y,c)}{LP_{Tot}(y,c)} + ImpFood_{Ant}(y,c)$$

Where $ImpFood_{Ant}(y,c)$ was calculated with Equation **S24** and $SelfProducedFood(y,c)$ was calculated as the total food consumed minus the imported food, both derived from FAOSTAT.

*Equation S24 – Anthropogenic P in imported food*

$$ImpFood_{Ant}(y,c) = \sum_{k=1}^{N}\sum_{i=1}^{25} ImpFood(y,c,k,i).concP(i).\frac{LP_{Ant}(y,k)}{LP_{Tot}(y,k)}$$

# 4 Calculation of Imported Feed and Food quantities

In this section we explain how we calculated $ImpFeed(y,c,k,i)$ and $ImpFood(y,c,k,i)$ used in Equation **S20** and Equation **S24**.

## 4.1. Imported Feed

The calculation of imported feed $ImpFeed(y,c,k,i)$ kg DM was done differently for each of the three time periods considered ([1950-1960],[1961-1985],[1986-2017]), given that different dataset were available.

For the 1986-2017 period, the Detailed Trade Matrix (DTM) gathered detailed information on the trade of agricultural products between countries. We worked only with the imported flows. For each item considered, we computed $ImpFeed(y,c,k,i)$ with Equation **S25**. Because the DTM dataset did not specify whether the imported quantities $IQ_{DTM}(y,k,j)$ were consumed as feed or food, we had to estimate it ourselves, using the coefficient $\delta_{Feed}(i)$ (Table **S7**). The latter was equal to 1 when the imported products were used 100% as feed (this was the case of cake, soybeans for example), 0

when the imported products were used only as food and calculated with Equation **S26** when the items could be used for both. In Equation **S26**, we divided the total quantities of item *i* consumed as feed in the country *c*, at year *y*, by the Domestic Supply Quantity of item *i*. Thus that ratio was an estimate of the fraction of item *i* that was consumed as feed in the country *c*. We hypothesised that this ratio also applied to the imported quantities, yet we acknowledge that this assumption is very strong and might not prove true in some cases.

*Equation S25 – Imported feed for each traded item considered for the period 1986-2017*

$$ImpFeed(y,c,k,i) = \sum_{j=1}^{allsubitems(i)} IQ_{DTM}(y,c,k,j).\delta_{Feed}(i)$$

With *i* corresponded to the Items Aggregated as referred to in Table **S7**. Each item *i* corresponded to a list of sub items in the DTM dataset, referred to with index *j*.

*Equation S26 – Fraction of the imported quantities used as feed*

$$\delta_{Feed}(i,y,c) = \frac{Feed(y,c,i)}{DSQ(y,c,i)}$$

Sometimes we found that our estimate of imported feed, calculated based on data from the DTM was larger than the total feed consumption, calculated with the Food Balances dataset. In such cases we decided to trust the data of the total feed consumed because it was derived from FAOSTAT raw data with no modification from our side, contrary to the calculation of the imported feed.

For the 1961-1985 period, we used the data on imported agricultural products derived from the Food Balances (FB) dataset from FAOSTAT. We computed $ImpFeed(y,c,k,i)$ with Equation **S27**.

*Equation S27 - Imported feed for each traded item considered for the period 1961-1985 – in kgDM*

$$\forall y \in [1961-1985], \qquad ImpFeed(y,c,k,i) = IQ_{FB}(y,c,i).\delta_{Feed}(i,y,c).f_k(c,i)$$

Where $IQ_{FB}(y,c,i)$ was the amount of product *i* imported to country *c*, at year *y*, derived from the FB database. $f_k(c,i)$ referred to the fraction of item *i* imported quantities toward country *c* that came from the partner country *k*. We estimated $f_k(c,i)$ for each item item, for each country, based on the repartition of their partner countries when considering item *i* over the 1986-1991 five year period.

Finally, for the 1950-1960 period, we scaled down the imported feed data from 1961 based on the livestock density of each country, expressed in livestock unit.

### 4.2. Imported Food

For the trade of food products we used the same methodology, dataset and equations as for the trade of feed products, except for $\delta_{Food}(i,y,c)$ that we calculated with Equation **S28**.

*Equation S28 – Fraction of the imported quantities used as food*

$$\delta_{Food}(i,y,c) = \frac{Food(y,c,i)}{DSQ(y,c,i)}$$

Where $Food(y,c,i)$ referred to the total quantities of item *i* consumed as food in the country *c*, at year *y* and was derived from the FB dataset (FAOSTAT).

## 5 Land expansion/abandonment

In our calculations we computed the effects of agricultural lands expansion/abandonment on the size of the P pools.

When agricultural area decreased, the size of the four soil P pools (in kgP.ha$^{-1}$.yr$^{-1}$) did not change. When agricultural area increased, we calculated the size of each agricultural soil P pool (X) with Equation **S29** and Equation **S30**.

*Equation S29 – Changes in the size of anthropogenic P pools following land expansion*

$$\forall X \in \{LP, SP\}, \qquad X_{Ant}(y,c) = \frac{X_{Ant}(y-1,c).A(y-1,c)}{A(y,c)}$$

*Equation S30 - Changes in the size of natural P pools following land expansion*

$$\forall X \in \{LP, SP\}, \qquad X_{Nat}(y,c) = \frac{X_{Nat}(y-1,c).A(y-1,c) + X_{Nat}(1961,c).\Delta A(y-1,c)}{A(y,c)}$$

Where *A* is the agricultural land (in ha), $\Delta A(y-1,c)$ is the difference between agricultural area at year *y* and at year *y-1*. LP and SP refers respectively to the labile and stable P pools (in kgP.ha$^{-1}$).

## 6 Calibration: methodology and results

### 6.1. Methodology of the calibration procedure

The calibration procedure aimed at calibrating the parameters $\beta$, $\gamma$ and $\mu_{SPtoLP}$ for each country. This procedure consisted of three steps and was done independently for each country.

Step 1: We defined ranges of possible values for each parameter. For $\beta$, which stands for the maximum attainable yield without any P limitation, we tested the following values: 1, 2, 3, 5, 7, 10 ,13, 15, 17, 20, 23, 25, 27, 30, 33, 35 kgP.ha$^{-1}$.yr$^{-1}$. Note that $\beta$ could not be lower than the minimum

value of the P harvest time series for each country. Thus the lowest value of $\beta$ tested for each country was country-dependant. For $\mu_{SPtoLP}$, which stands for the turnover rate of the stable P pool, we tested the following values: 0.009, 0.01, 0.02, 0.03, 0.04, 0.05, 0.06, 0.07, 0.08, 0.09, 0.1, 0.2, 0.3, 0.4, 0.5, 0.6, 0.7, 0.8, 0.9 $yr^{-1}$. This corresponds to mean residence time of P in the stable pool ranging from 111 years to 1 year. The range we tested is very large compared to data found in the literature (Table **S1**), but we wanted to be as broad as possible given the diversity of the pedo-climatic conditions at the global scale.

*Table S1 - Turnover rates of the stable pool found in the literature*

| Sources | Ranges in literatures | Spatial scale |
|---|---|---|
| (Sattari et al., 2012) | 0.04<br>(sensitivity analyses: 0.025 – 0.08) | Defined for each world region |
| (Ringeval et al., 2014) | 0.035–0.070 | France |
| (Zhang et al., 2017) | Calculated based on the size of the P pools and on the turnover rate of the labile pool. Final range not provided. | World: spatially explicit analyses |
| (Le Noë et al., 2020) | 0.005-0.1 (mean: 0.02) | France – Calibrated for each French region based on P Olsen observations |

For $\gamma$, which depicts the ability of crops to extract soil P, the range of values to test was more difficult to define. We chose to start from the range of values provided in (Ringeval et al., 2014) and decided to extend it by several order of magnitude. As a result, we tested for each country the following values: 0.00001, 0.00003, 0.00005, 0.00009, 0.0001, 0.0003, 0.0005, 0.0007, 0.0009, 0.001, 0.002, 0.003, 0.004, 0.005, 0.006, 0.007, 0.008, 0.009, 0.01, 0.03, 0.05, 0.07, 0.09, 0.1, 0.2, 0.5, 0.9 $ha.kgP^{-1}$.

Step2: For each country, we combined these three parameters into triplets and run the model for each of them. For each simulation output we computed two calibration scores (see Equations **4** and **5** of the main text) and selected triplets based on these scores.

Score 2 was calculated with $LP_{obs}$ values derived from (Ringeval et al., 2017) (main calibration, the results of which are presented in the main text) or with $LP_{obs}$ values derived from datasets gathering measurements of P availability in agricultural soils for few countries (see section **S2.7.2**) (second calibration, the results of which are only presented in the Supplementary information, see Section **S6.3**).

As part of the main calibration, we evaluated how the uncertainty related to the labile P pools provided by (Ringeval et al., 2017) propagated to the calibrated parameters. For each triplet and

corresponding simulation outputs, we computed the score 2 three times with the $LP_{obs}(2005)$ value respectively equal to (i) the labile pool mean value coming from Ringeval et al. 2017, (ii) the mean value minus the standard deviation coming from Ringeval et al. 2017 and (iii) the mean value plus the standard deviation.

Step 3: We selected triplets of parameters based on the obtained calibration scores. If at least one triplet of parameters match (constraint 1) score 1 + score 2 < 30%, we kept all triplets that matched this constraint. If no triplets matched constraint 1 but some match score 1 < 30% (constraint 2), we kept the ones that matched this second constraint. Elsewhere, no triplets were kept and the corresponding countries were not further studied (category 3). Countries that matched constraint 1 joined the category 1, while those that matched the constraint 2 joined the category 2.

Uncertainty provided for the signatures in the main text has two origins: one related to $LP_{obs}(2005)$ used in step 2 (mean, mean+std, mean-std); and one related to the different triplets selected in step 3 for a given $LP_{obs}(2005)$.

## 6.2. Results from the main calibration procedure

The results from the calibration procedure are presented in Figure **S3**. 62% of the countries studied presented a score 1+ score 2 ≤ 30%. For these countries the model was adequate to simulate the P harvest available data and the size of the labile pool provided by (Ringeval et al., 2017). 29% of the countries, mainly located in Africa, had a score 1+score 2 > 30% but a score 1 ≤ 30%. For these countries the model managed to reproduce the temporal trends of soil P harvest but struggled to match the labile pool simulated size with the labile pool value derived from (Ringeval et al., 2017). This can be explained by different methodologies used in (Ringeval et al., 2017) and in this paper to calculate the initial size of the labile pool. In their work, (Ringeval et al., 2017) initialized the size of their labile pool with the data on natural soil P derived from the Hedley fractionation measures by (Yang et al., 2013). Here, we initialized the size of the labile pool based on the available information on the P harvest in 1950 using Equation **2** (main text). If the labile pool derived from 1950 P harvest was too far to Yang et al soil P pools, our calibration procedure cannot match the two constraints (on export and soil P) at the same time. For the remaining countries (7% of countries - including Cuba, Estonia, Jordan, Kazakhstan, Latvia, Lithuania, Tajikistan, Turkmenistan, and Ukraine) no triplet matched any of the two constraints. For these countries our model did not prove adequate to reproduce observed trends in the soil labile pool and in the P harvest from agricultural lands.

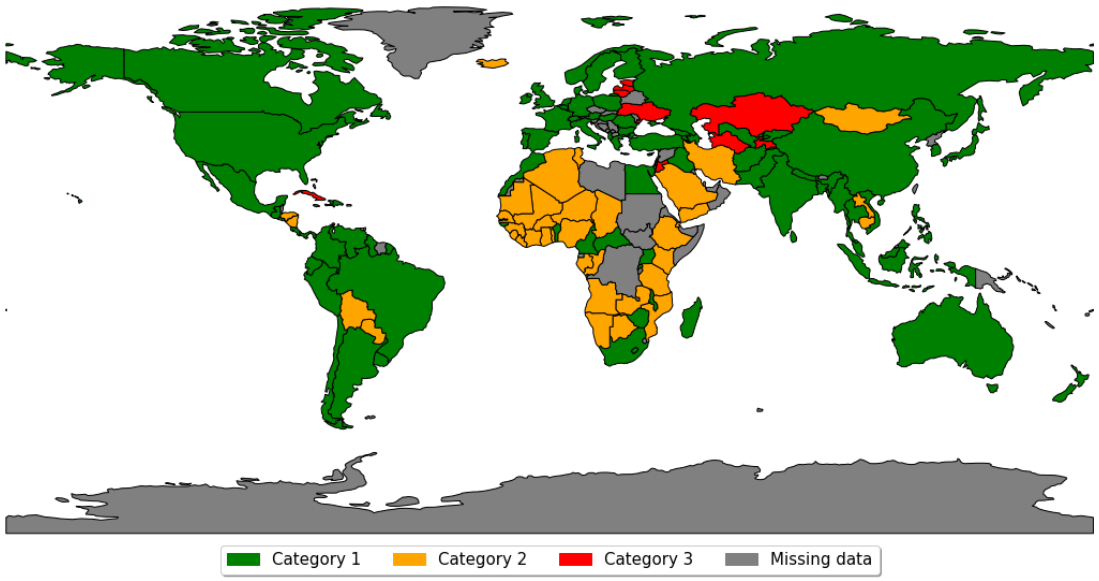


*Figure S3 – Countries classification based on the outputs from the calibration procedure. Category 1 gathers countries for which score 1+ score 2 ≤ 30%. Category 2 gathers countries for score 1+ score 2 > 30% but score 1 ≤ 30%. Category 3 includes countries for which none of the above constraints was met. Data are displayed per country. Countries coloured in grey were excluded from the calculation because of missing data (as for Democratic Republic of Congo, Libya and Somalia among others).*

The calibrated values for the three parameters are shown in Figures **S8-S13**. Globally, $\beta$ ranged from 12 ±9 for Afghanistan to 32 ±2 kgP.ha$^{-1}$.yr$^{-1}$ for Bangladesh. The values of $\mu_{SPtoLP}$ showed larger differences between countries, and were associated with large uncertainties as well. It varied from 0.010 ±0.003 for Jamaica to 0.811 ±0.099 yr$^{-1}$ for Rwanda. At the global scale, $\gamma$ ranged from 0.0001 ± 0.0001 for Peru to 0.0714 ±0.0811 ha.kgP$^{-1}$ for Sierra Leone.

Country-specific results of the calibration are provided in Figures **S20-S26**.

## 6.3. Result of the second calibration - with observed data used to constraint the size of the labile P pool

In Figure **S4** we compared the anthropogenic signatures of the labile P pool when triplets were selected with the main calibration vs. when they were selected with the second calibration. As a reminder, in the main calibration, the size of the labile pool was constraint (score 2) based on the available data from Ringeval et al. 2017, while in second calibration the size of the labile pool was constraint based on measured data on the soil P fertility of agricultural soils derived from different databases (see Section **S2.7**).

For all countries we found small differences in the anthropogenic signature whatever the calibration method used.

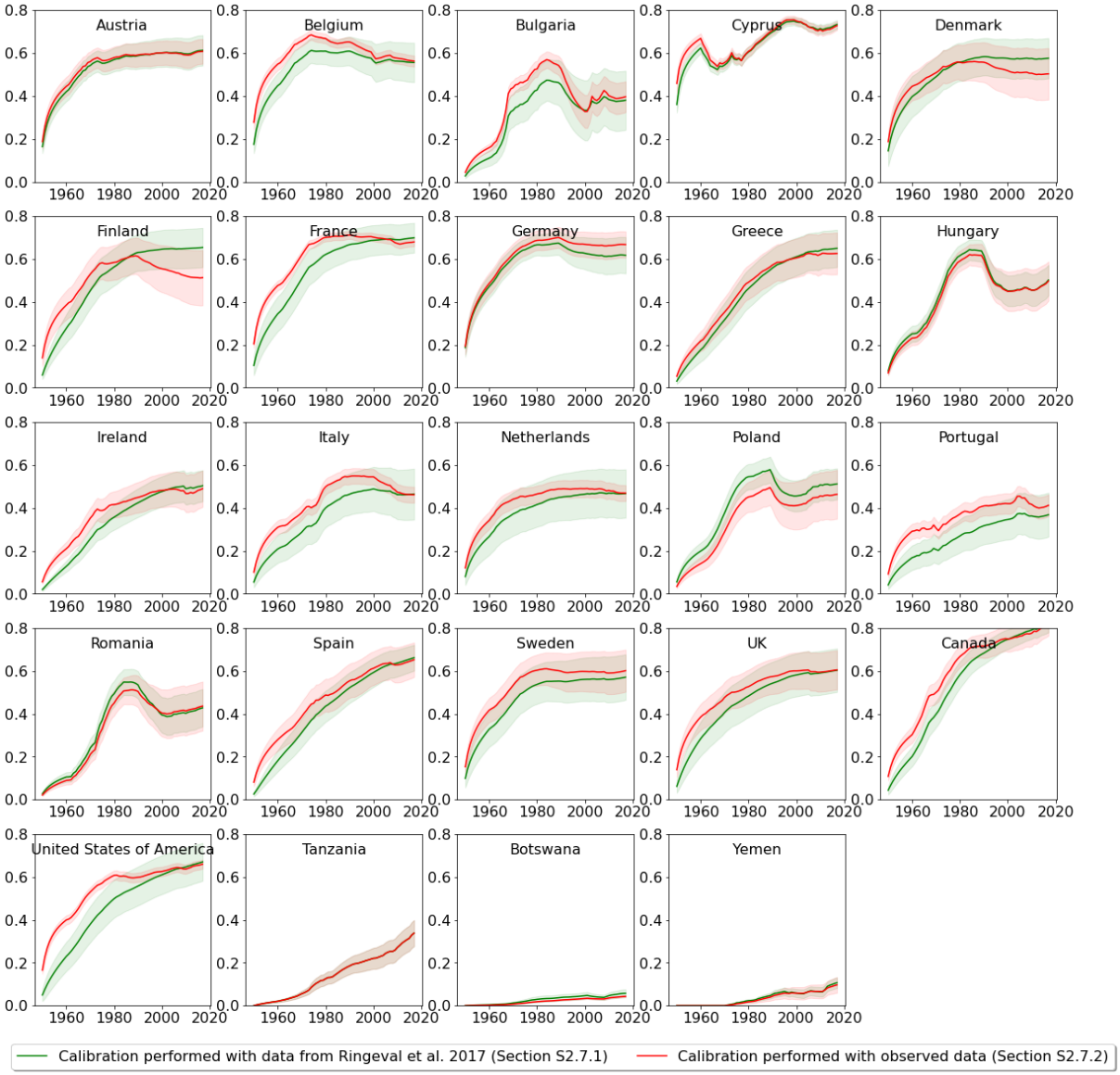


*Figure S4 – Comparison of anthropogenic signature of the soil labile P pool when the calibration was performed with $LP_{obs}$ data derived from Ringeval et al. 2017 (main calibration – in green) or with $LP_{obs}$ data from soil P tests we collected from the literature (in red).*

# 7 Data analysis

For each country, the mean and standard deviation value of the anthropogenic signature of their soil P pools were computed based on the outputs from our simulations for all the calibrated triplets. Thus the standard deviations reflect the uncertainties from the three calibrated parameters and from the size of the labile P pool used to constraint the model.

To calculate the average anthropogenic signature (± standard deviation) per world region, we computed weighted averages of the values (± standard deviation) per country. The weighting was calculated based on the average agricultural area of each country.

# 8 Main drivers of the values and temporal evolutions of the soil P anthropogenic signatures

For each country we were able to approach the simulated temporal evolution of anthropogenic signature of soil P pools thanks to few variables, underlying the key role played by these variables in the simulated signatures. We show that the anthropogenic signature of the stable P pool could be explained by (i) the cumulated use of mineral P fertilizer over the 1950-2017 period and (ii) its initial soil P content in 1950 (Figure **S5**, Equation **S31**). In comparison, the anthropogenic signature of the labile P pool was in addition to the two factors mentioned above, also dependant on (iii) the P transfers between the P pools.

## 8.1 Drivers of the anthropogenic signatures of the total soil P pools

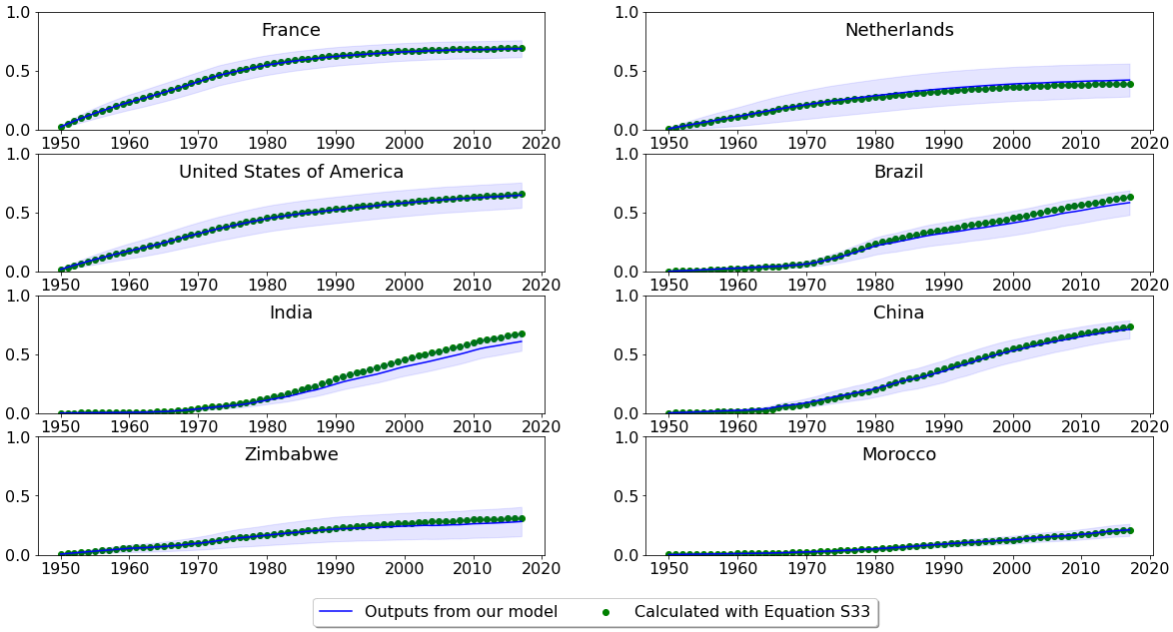


*Figure S5 – Temporal evolution of the anthropogenic signature of total soil P over the period 1950-2017 for 8 contrasting countries. In blue: anthropogenic signature of total soil P (mean and standard deviation) obtained from our simulations. In green: the anthropogenic signature of total soil P calculated with Equation S31*

*Equation S31 - Anthropogenic signature of total soil P calculated based on the cumulated application of mineral P fertilizers and the initial size of the P pools in 1950*

$$EstimatedSignAnt_{P_{Tot}}(y) = \frac{1}{M}\sum_{k=1}^{M}\frac{\sum_{i=1}^{y} CF(i)}{\sum_{i=1}^{y} CF(i) + P_{Tot}(1950,k)}$$

Where *k* refers to a given triplet and *M* is the total number of triplets selected for country *c*. $P_{Tot}$ is the sum of labile and stable P pools.

## 8.2 Drivers of the anthropogenic signatures of the soil labile P pool

In Figure **S6**, we plotted together the anthropogenic signature of the soil labile P pool derived from our simulations and the anthropogenic signature of the soil labile P pool calculated with Equation **S32**. The mismatch between the two curves shows that the cumulated use of mineral P fertilizers over the whole study period and the initial size of the labile pool in 1950 were not enough to explain the values derived from our simulations.

We had anticipated that the P transfers between the pools would also influence the anthropogenic signature of the soil labile P pool. As a result, we run new simulations in which we cancelled the P transfers between the pools. The values we obtained (Figure **S7**) shows that indeed soil P dynamics also influenced the anthropogenic signature of the soil labile P pool.

*Equation S32 - Anthropogenic signature of soil labile pool calculated based on (i) the cumulated application of mineral P fertilizers, and (ii) the initial size of the P pools in 1950*

$$EstimatedSignAnt_{LP_{Tot}}(y) = \frac{1}{M}\sum_{k=1}^{M}\frac{\sum_{i=1}^{y} CF(i)}{\sum_{i=1}^{y} CF(i) + LP_{Tot}(1950,k)}$$

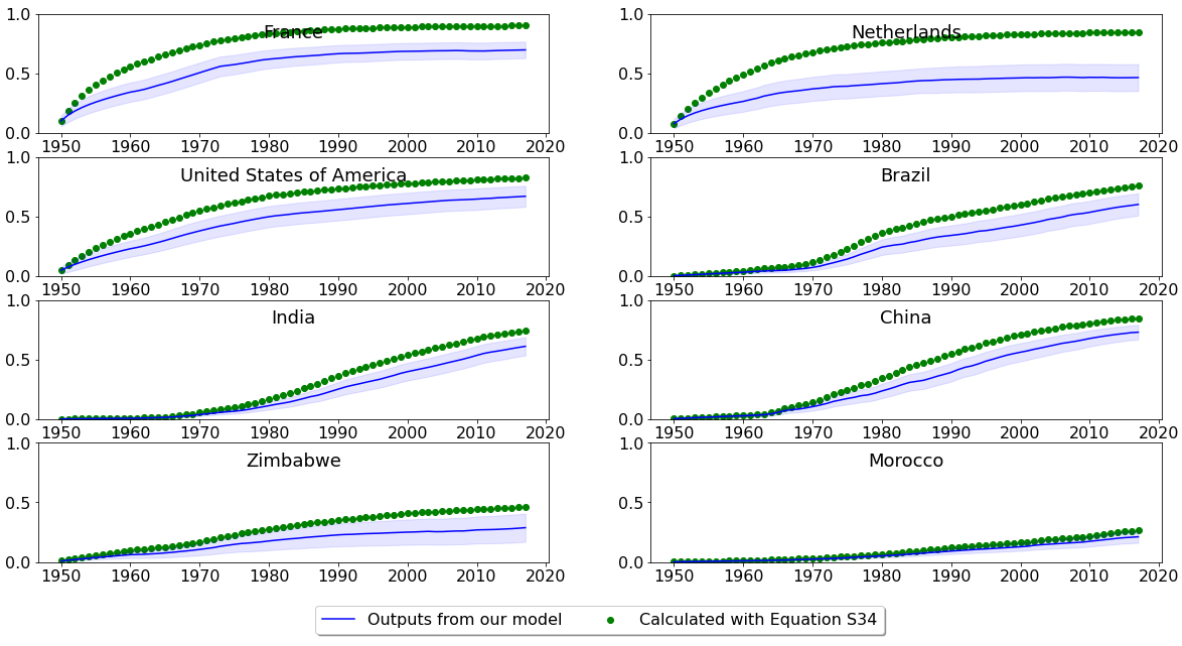


*Figure S6 - Temporal evolution of the anthropogenic signature of the soil labile P pool over the period 1950-2017 for 8 contrasting countries. In blue: anthropogenic signature of the soil labile P pool (mean and standard deviation) obtained from our simulations. In green: the anthropogenic signature of the soil labile P pool calculated with Equation S32.*

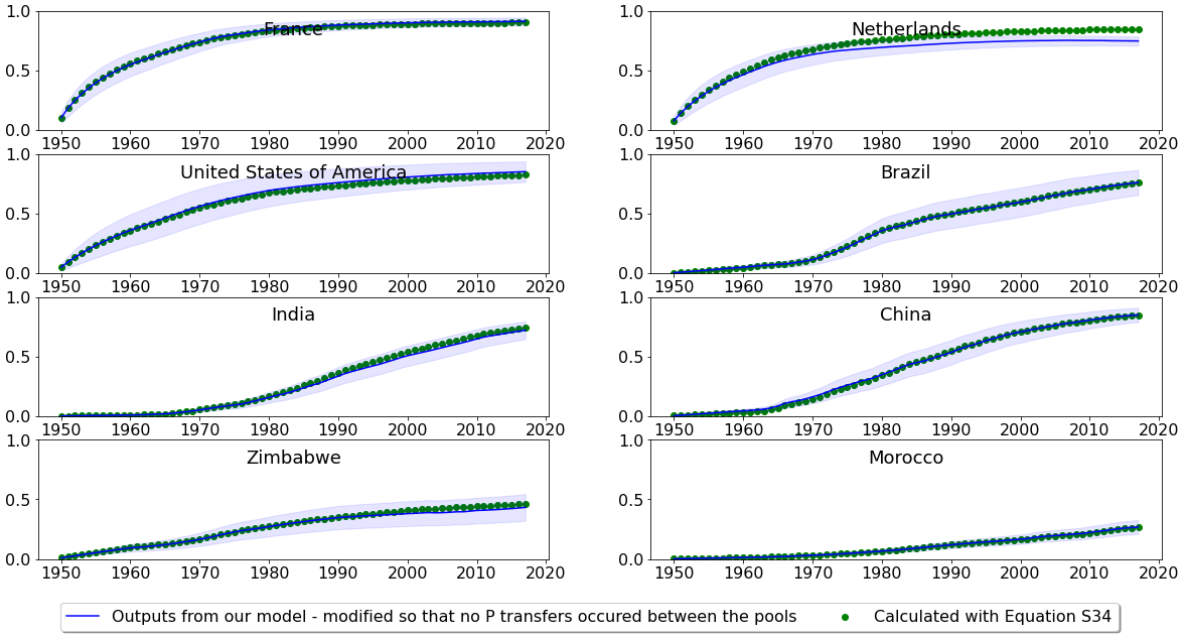


*Figure S7 – Temporal evolution of the anthropogenic signature of the soil labile P pool over the 1950-2017 period for 8 contrasting countries after suppressing the P transfer between soil pools. In blue: anthropogenic signature of the soil labile pool (mean and standard deviation) obtained from our simulations, in which we set the P transfers between the pools to zero. In green: the anthropogenic signature of the soil labile pool calculated with Equation S32.*

# 9 Estimates of the size of the soil labile and stable P pools

The sizes of soil labile and stable P pools were estimated for each country from 1950 to 2017 - with a yearly time step. The sizes of the P pools in 2017 resulted both from our estimate of the P pools sizes in 1950 and soil P inputs, outputs and dynamics over the study period. Estimates of the size of the labile P pool in 1950 were derived from available data on soil P harvest in 1950 (see Equation **2**). It was also function of the calibrated values of $\beta$ and $\gamma$. The size of the stable P pool in 1950 was calculated based on that of the labile P pool in 1950 assuming an equilibrium between the two pools (see Equation **3**, T=0). As a result, the size of the stable P pool was very sensitive to the value of the calibrated parameter $\mu_{SPtoLP}$.

Overall our estimates of the P pool sizes in 1950 and throughout the study period displayed large uncertainties (shown only for year 1950 - see Figures **S18** and **S30**-**31**). The uncertainties we computed reflect uncertainties both in the calibration of the model parameters (see Section **S6**) and in the size of the labile P pool used to constraint the model (see Section **S2.7**). Figures **S30-31** show larger initial (i.e. in 1950) soil P pools in our approach for Western Europe than for the rest of the world. This difference could also be found in (Ringeval et al., 2017) and were explained by differences in soil biogeochemical background and in farming practices – mainly as manure - before 1950.

We propagated the uncertainties we found on the size of the P pools on our anthropogenic signature estimates and the obtained errors were reasonable (Figure **S14**).

## Supplementary Figures

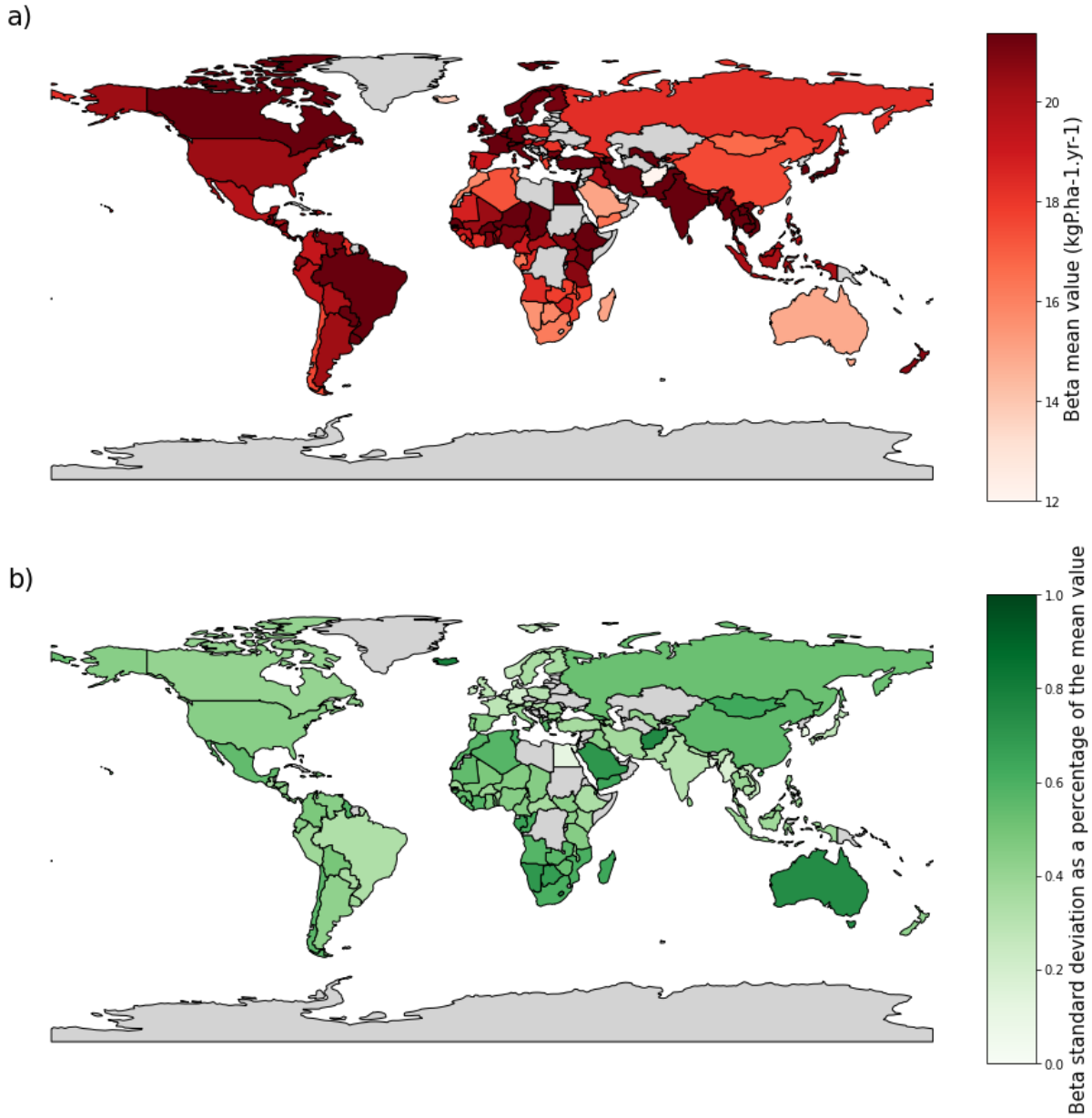


*Figure S8 – Calibrated values of β (mean- a) and standard deviation (as a percentage of the mean value - b) for all countries in category 1 and 2.*

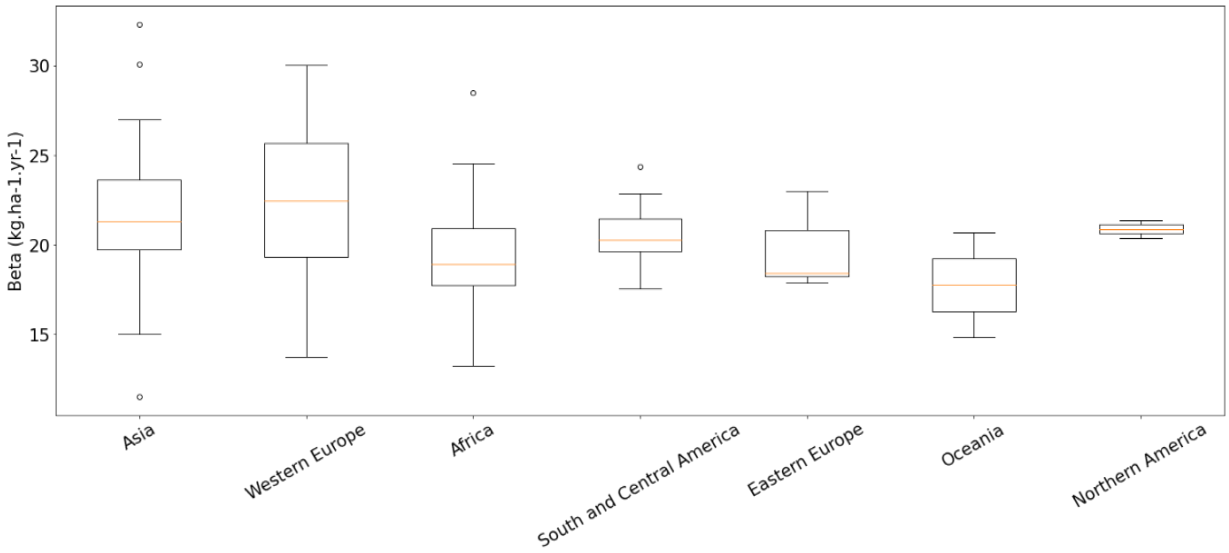


*Figure S9 – Distribution of the mean calibrated values of β for each world region considered.*

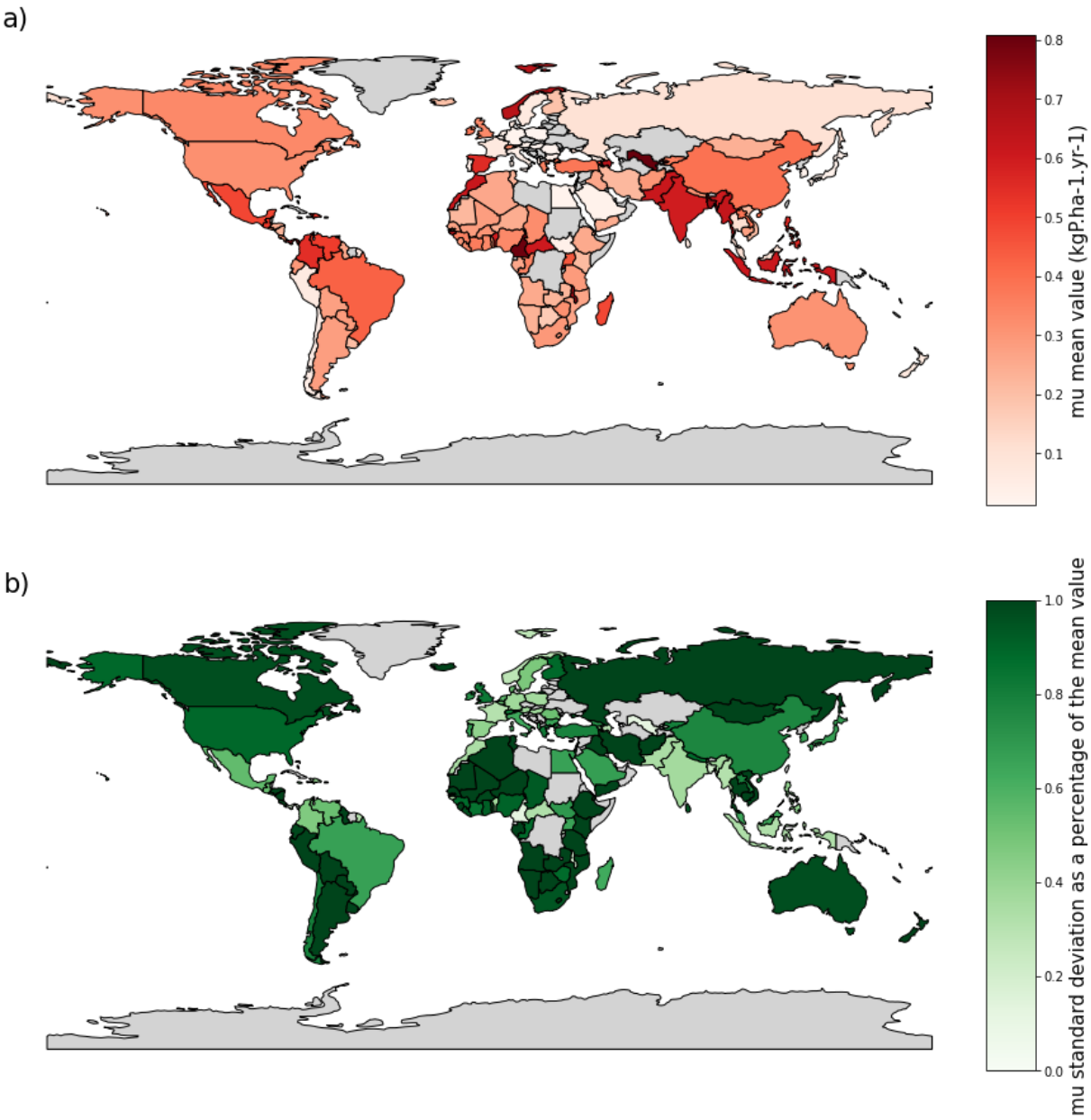


*Figure S10 - Calibrated values of $\mu_{SPtoLP}$ (mean- a) and standard deviation (as a percentage of the mean value - b) for all countries in category 1 and 2.*

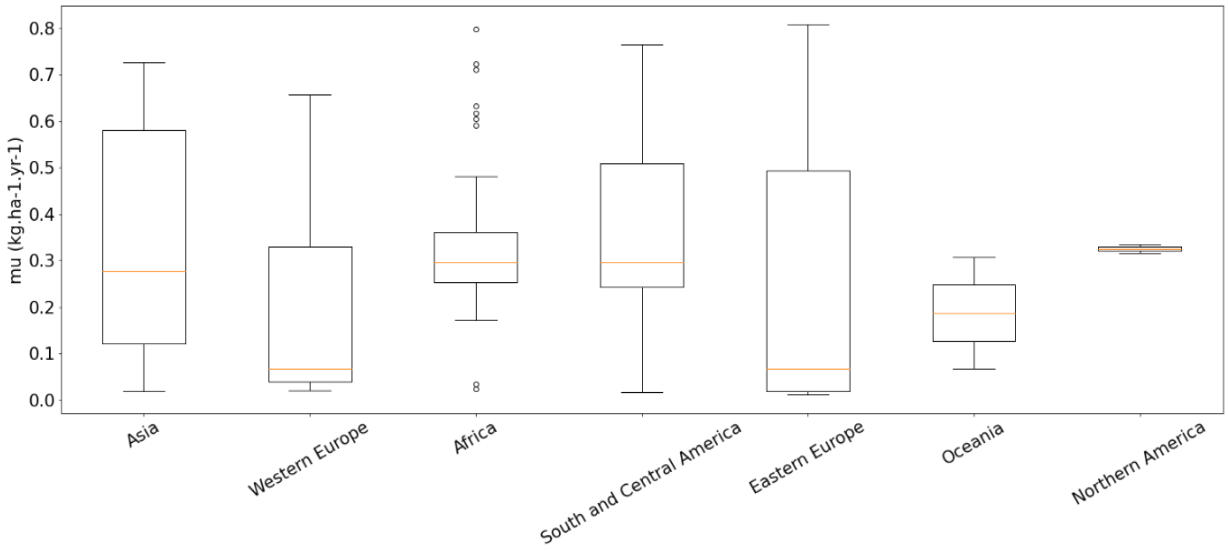


*Figure S11 - Distribution of the mean calibrated values of $\mu_{SPtoLP}$ for each world region considered.*

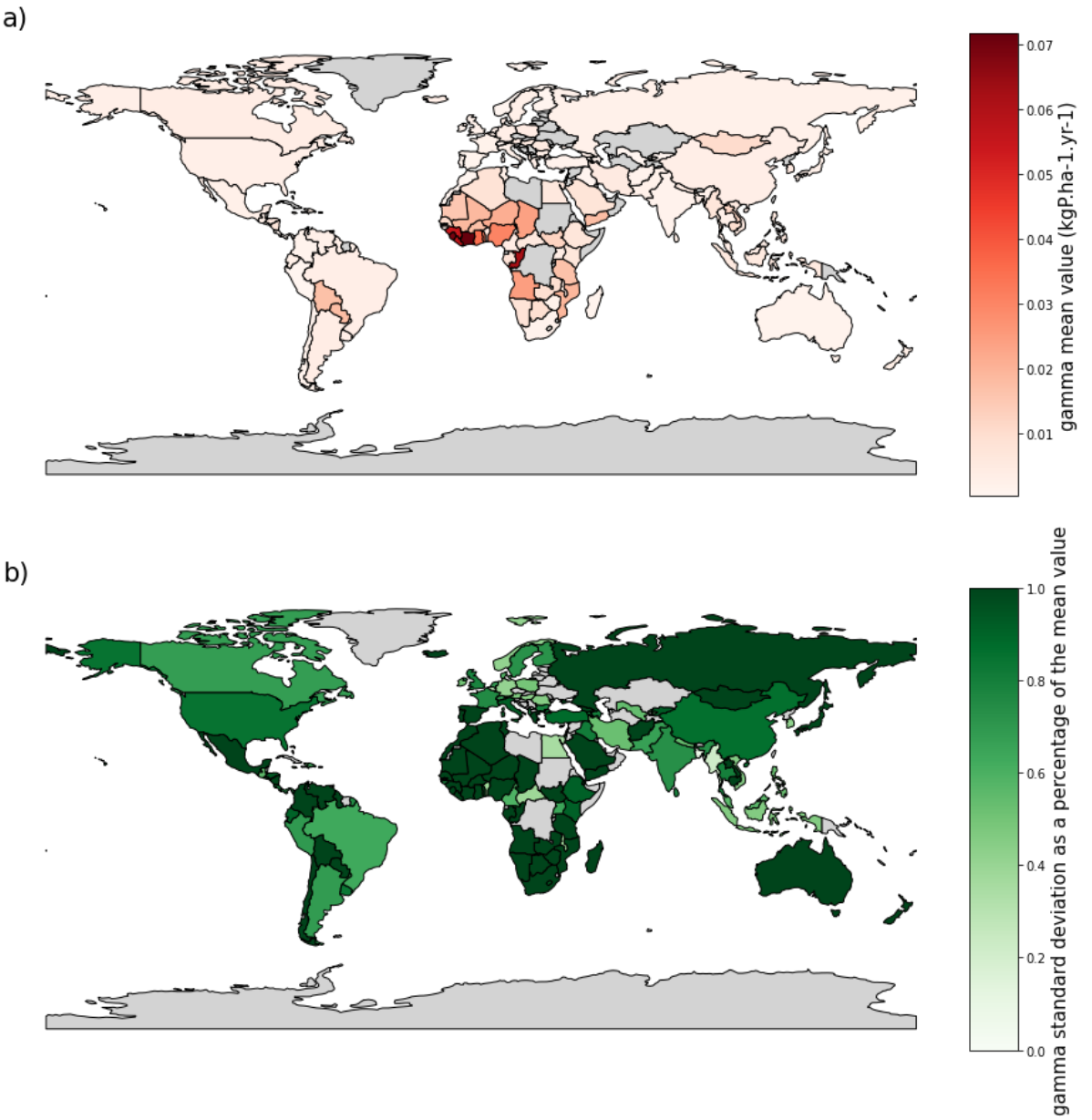


*Figure S12 - Calibrated values of γ (mean- a) and standard deviation (as a percentage of the mean value –b) for all countries in category 1 and 2.*

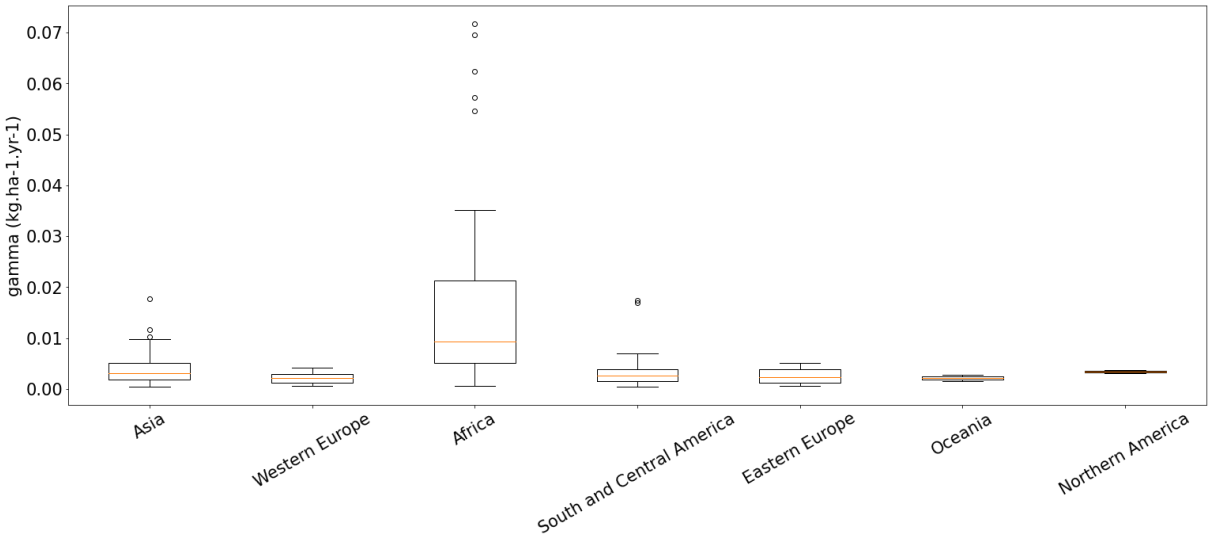


*Figure S13 - Distribution of the mean calibrated values of γ for each world region considered.*

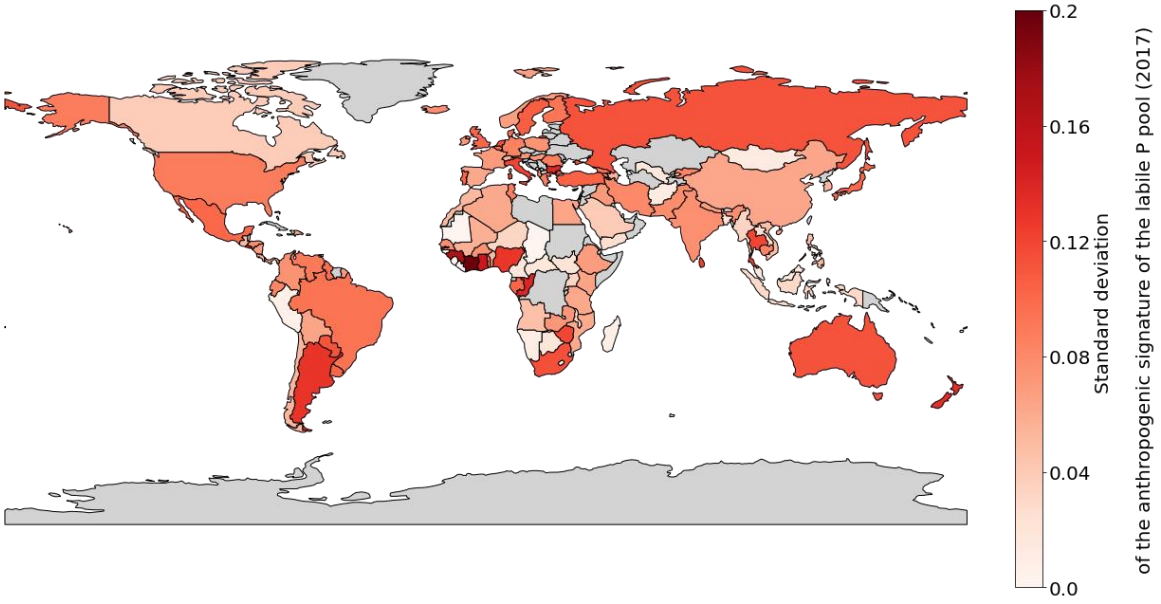


*Figure S14 – Standard deviations of the soil labile pool anthropogenic signatures in 2017. Countries in grey correspond to countries for which data were missing and countries from category 3 for which we did not compute the anthropogenic signatures.*

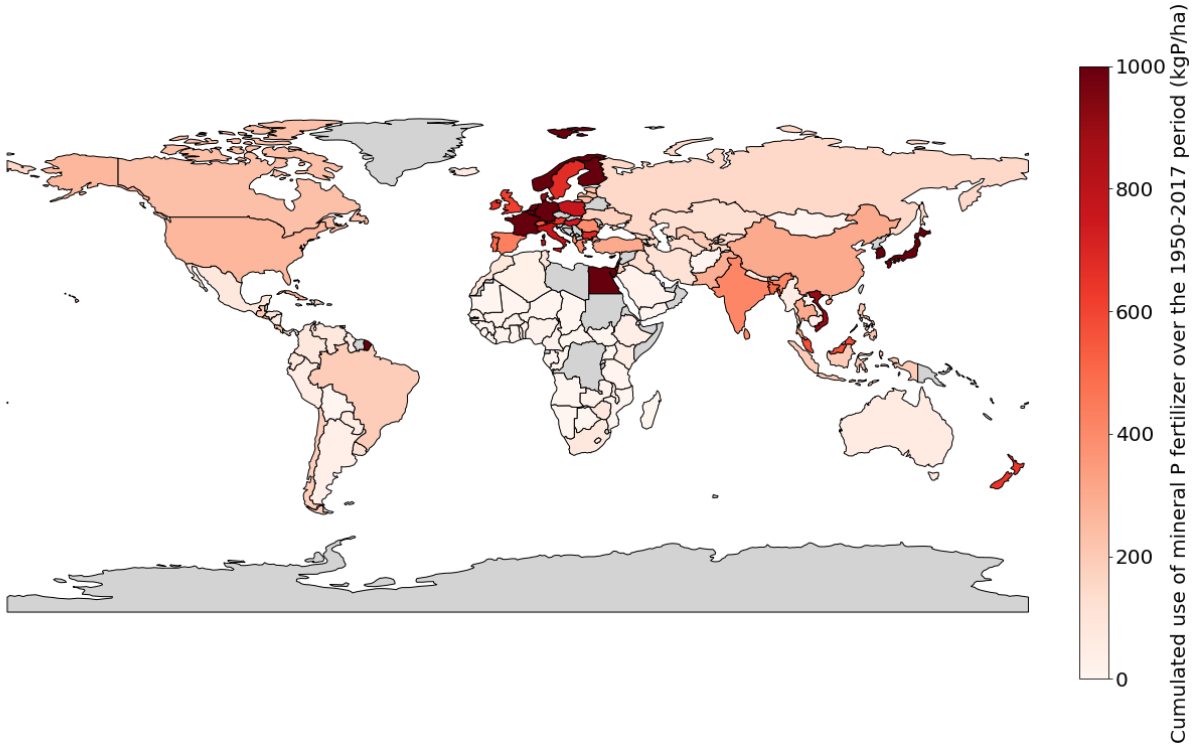


*Figure S15 - Cumulated application of mineral P fertilizer (CF) over the 1950-2017 period for each country. Data are in kgP.ha$^{-1}$.*

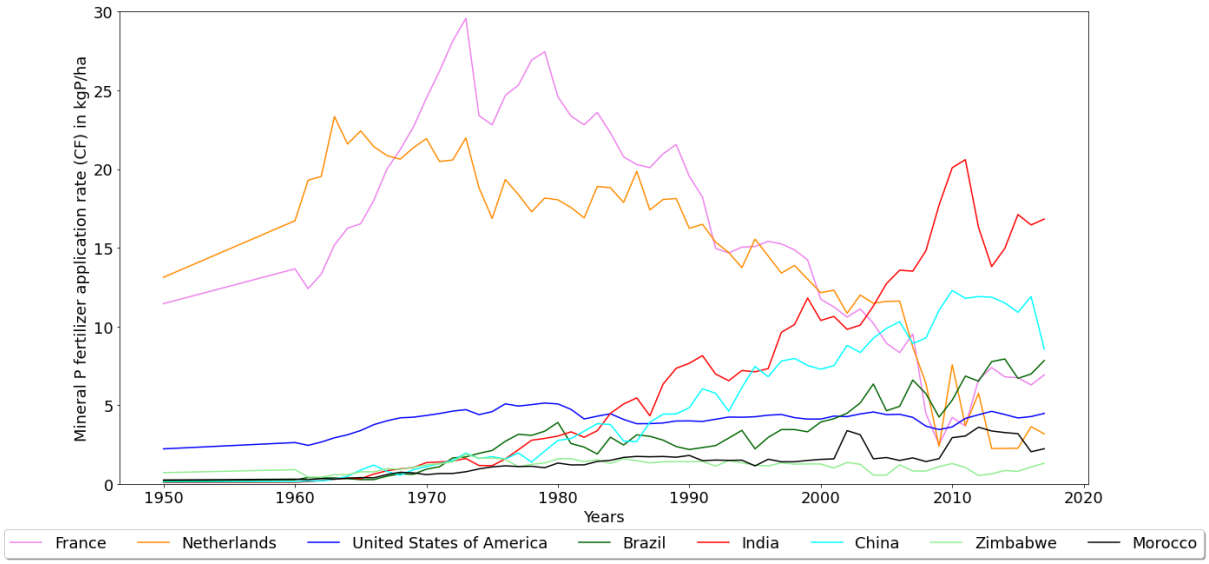


*Figure S16 – Inputs data analysis of the eight contrasting countries : temporal evolution of mineral P fertilizer application rates for the 1950-2017 period. Data are in kgP.ha$^{-1}$ applied on both croplands and grasslands.*

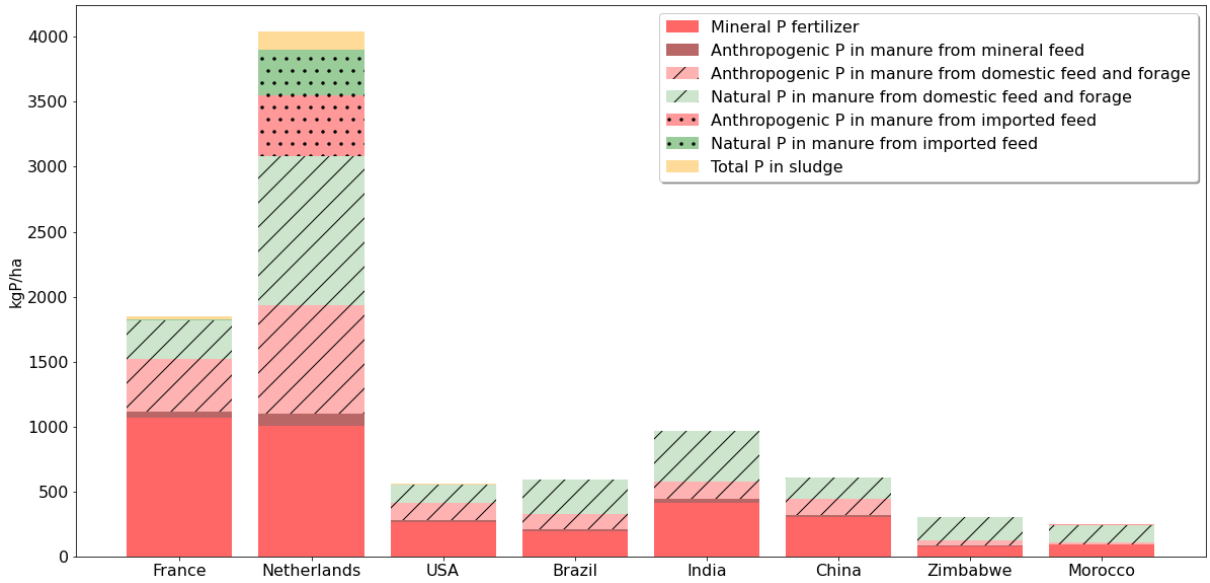


*Figure S17 – Soil cumulative P inputs for the 1950-2017 period with a distinction between anthropogenic and natural P fluxes. In red: anthropogenic P fluxes. In green, natural P fluxes. The flux of manure (OF) was split in 3 categories: (i) the manure that originated from the consumption of domestically produced feed (ii) the manure that originated from the consumption of imported feed and (iii) the manure that originated from the consumption of mineral feed. For clarity, we did not show the anthropic vs. natural origin of P embedded in sludge (in yellow), although they have been considered in the model.*

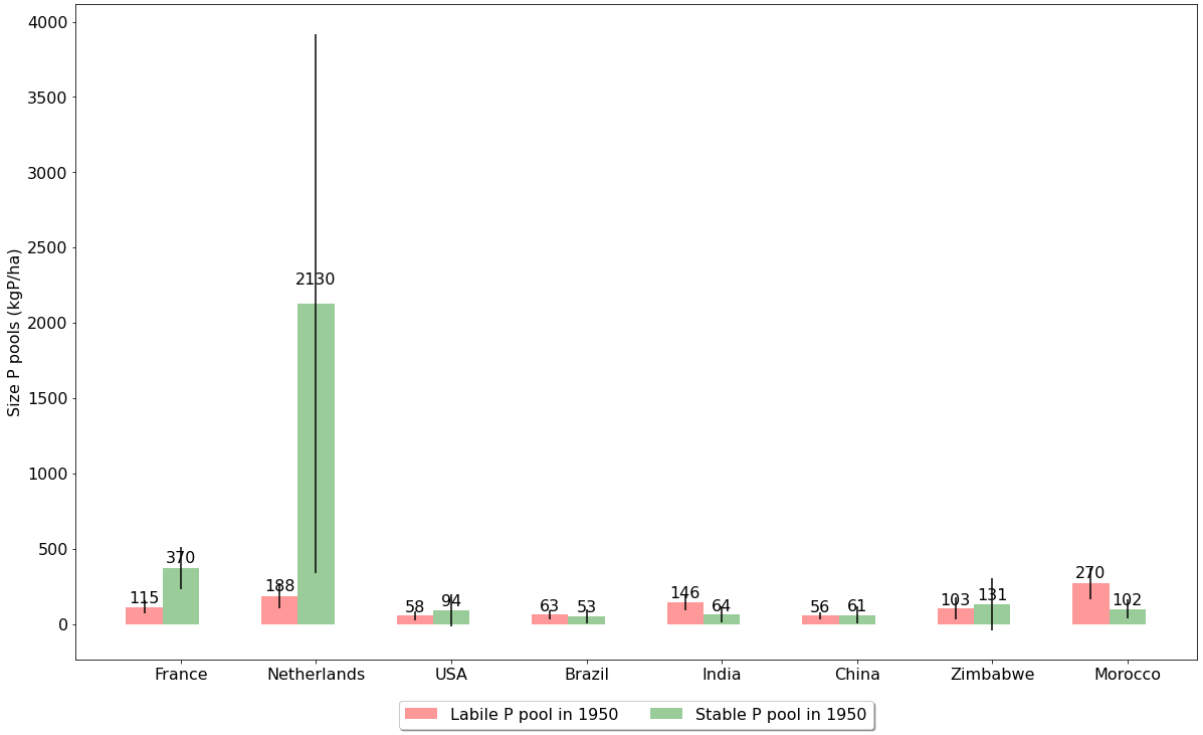


*Figure S18 –Estimate of the size of agricultural soil labile and stable P pools for eight contrasting countries in 1950. Mean and standard deviation values are provided.*

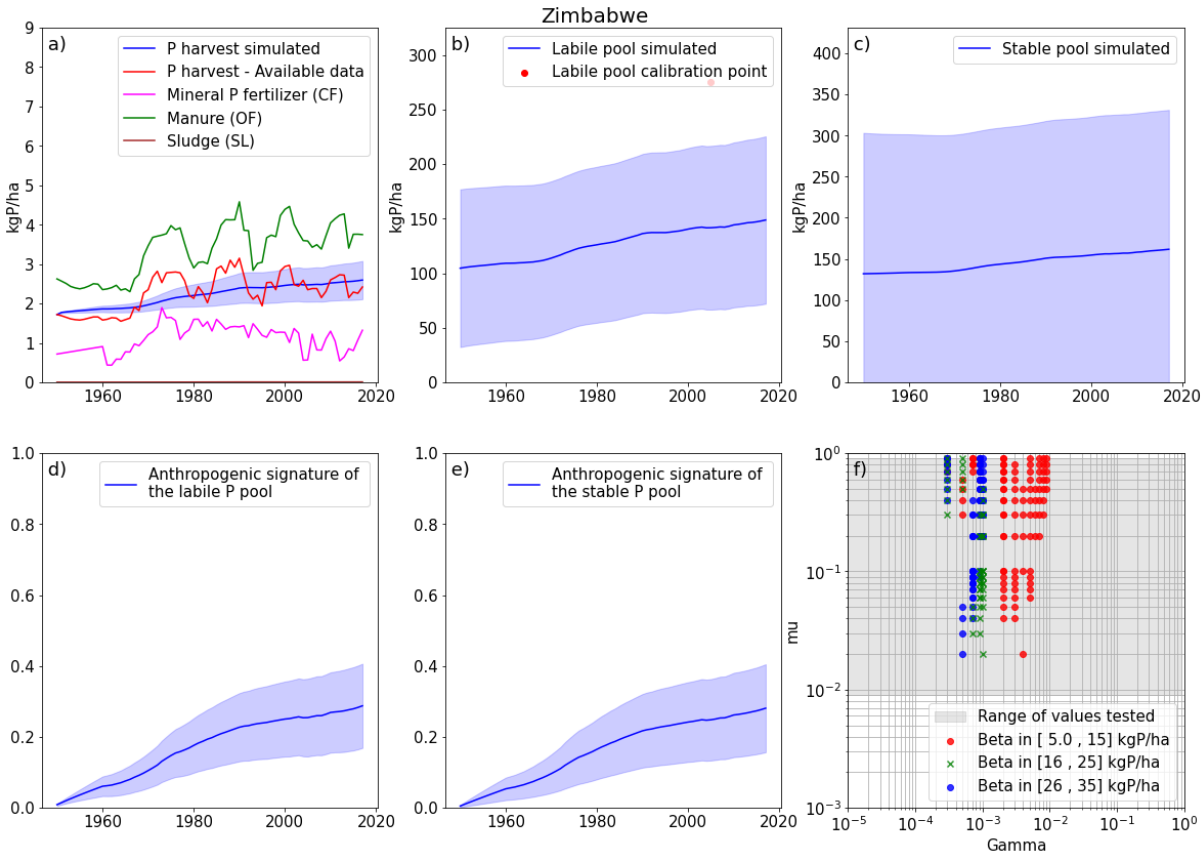


*Figure S19 – Country-specific results: case of Zimbabwe. From the top to the bottom and from the right to the left: (a) P harvest available information (red) and simulated one, inputs of mineral P fertilizer (pink) and manure (green), (b) Size of the labile pool in kgP.ha$^{-1}$, (c) size of the stable pool in kgP.ha$^{-1}$, (d) anthropogenic signature of the labile pool, (e) anthropogenic signature of the stable pool and (f) values taken by the three calibrated parameters following the calibration procedure. In blue are the simulated values, displayed with a mean value (bold line) and a standard deviation (light blue).*

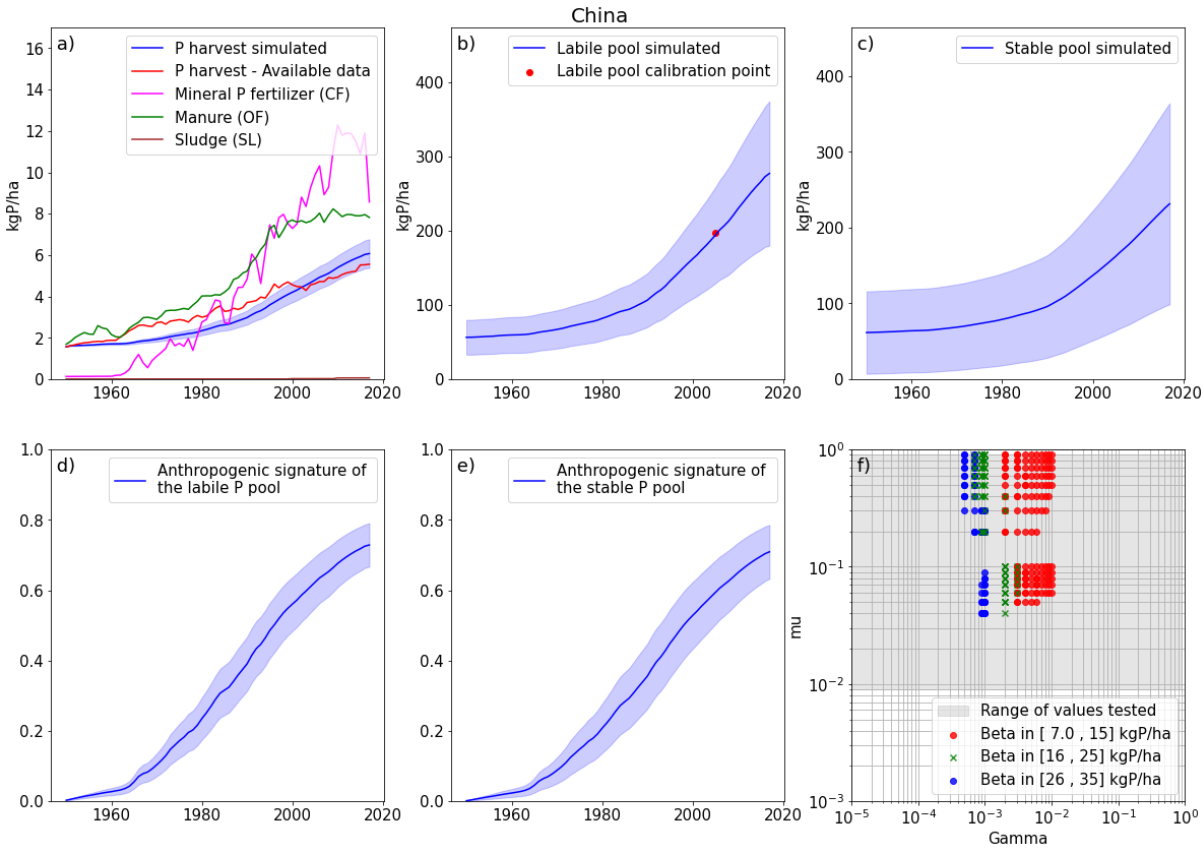


*Figure S20 - Country-specific results: case of China. From the top to the bottom and from the right to the left: (a) P harvest available information (red) and simulated one, inputs of mineral P fertilizer (pink) and manure (green), (b) Size of the labile pool in kgP.ha$^{-1}$, (c) size of the stable pool in kgP.ha$^{-1}$, (d) anthropogenic signature of the labile pool, (e) anthropogenic signature of the stable pool and (f) values taken by the three calibrated parameters following the calibration procedure. In blue are the simulated values, displayed with a mean value (bold line) and a standard deviation (light blue).*

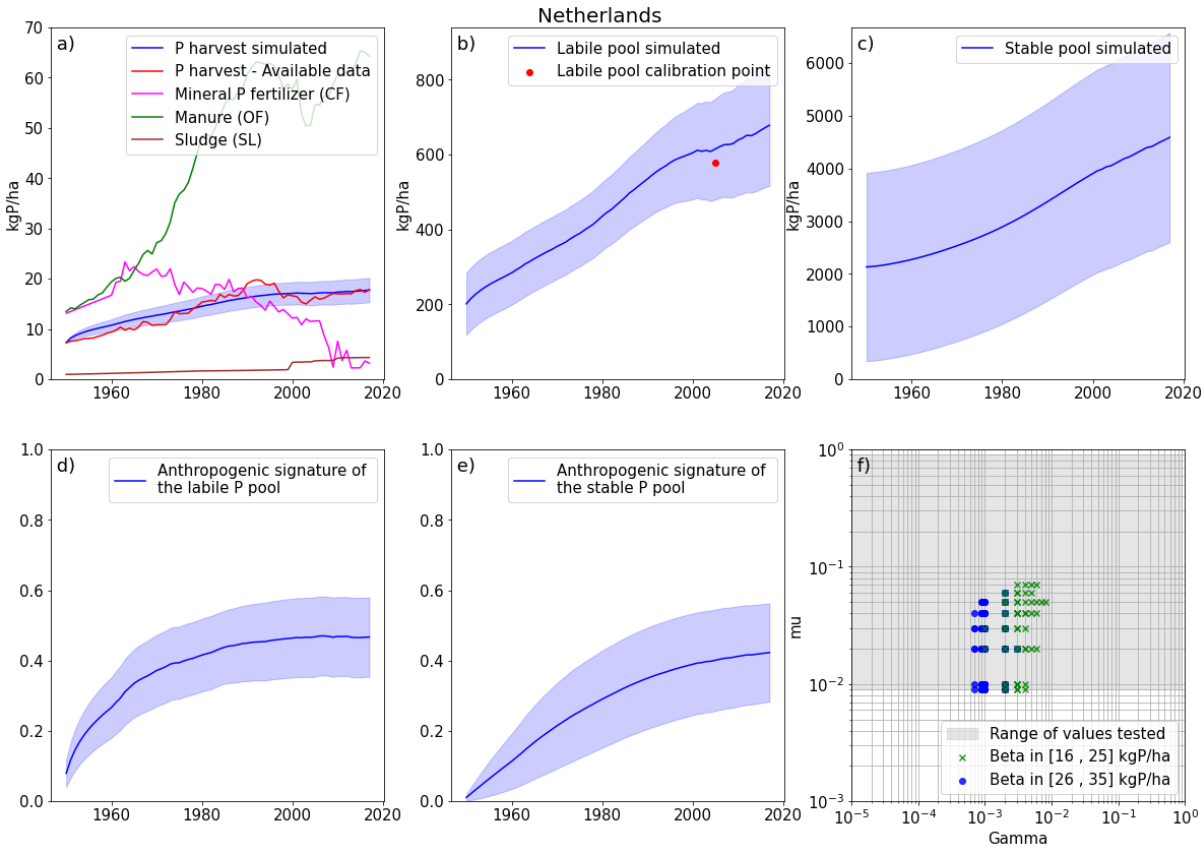


*Figure S21 - Country-specific results: case of the Netherlands. From the top to the bottom and from the right to the left: (a) P harvest available information (red) and simulated one, inputs of mineral P fertilizer (pink) and manure (green), (b) Size of the labile pool in kgP.ha$^{-1}$, (c) size of the stable pool in kgP.ha$^{-1}$, (d) anthropogenic signature of the labile pool, (e) anthropogenic signature of the stable pool and (f) values taken by the three calibrated parameters following the calibration procedure. In blue are the simulated values, displayed with a mean value (bold line) and a standard deviation (light blue).*

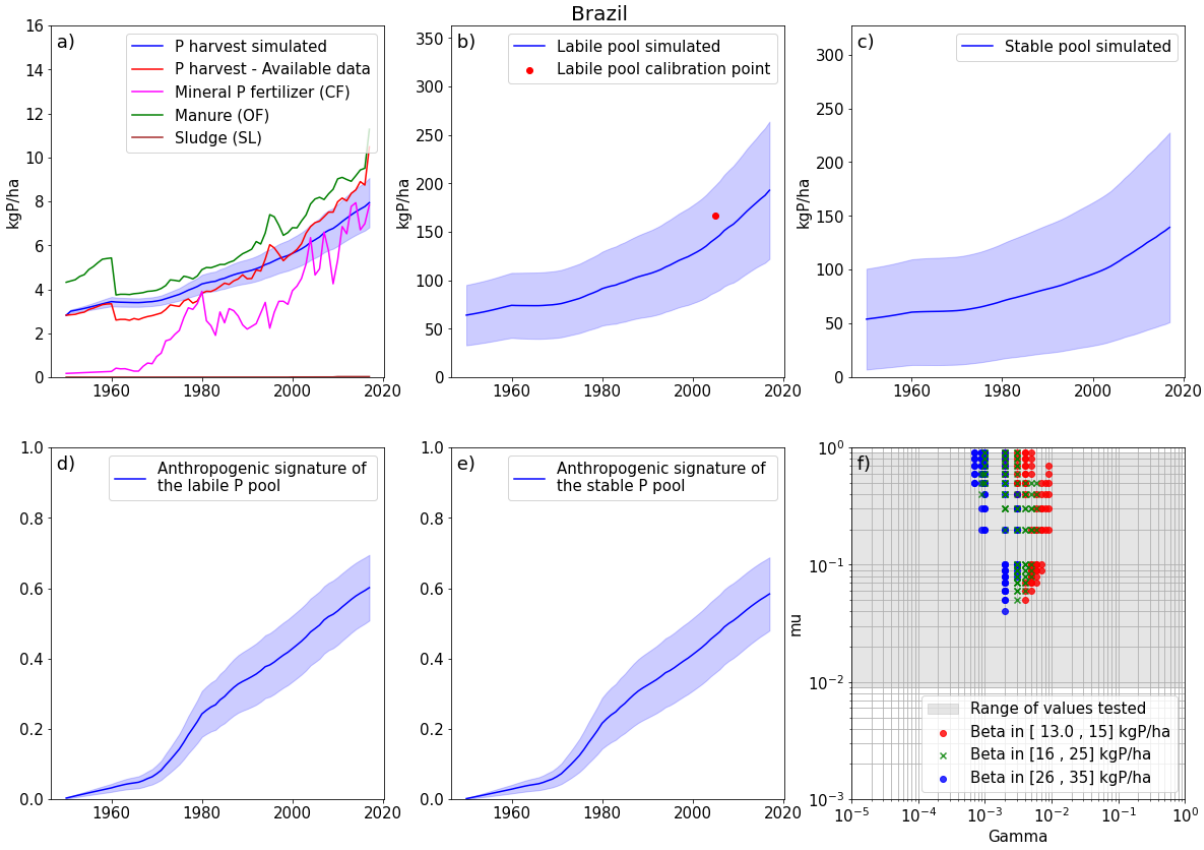


*Figure S22 - Country-specific results: case of Brazil. From the top to the bottom and from the right to the left: (a) P harvest available information (red) and simulated one, inputs of mineral P fertilizer (pink) and manure (green), (b) Size of the labile pool in kgP.ha$^{-1}$, (c) size of the stable pool in kgP.ha$^{-1}$, (d) anthropogenic signature of the labile pool, (e) anthropogenic signature of the stable pool and (f) values taken by the three calibrated parameters following the calibration procedure. In blue are the simulated values, displayed with a mean value (bold line) and a standard deviation (light blue). Case of Brazil.*

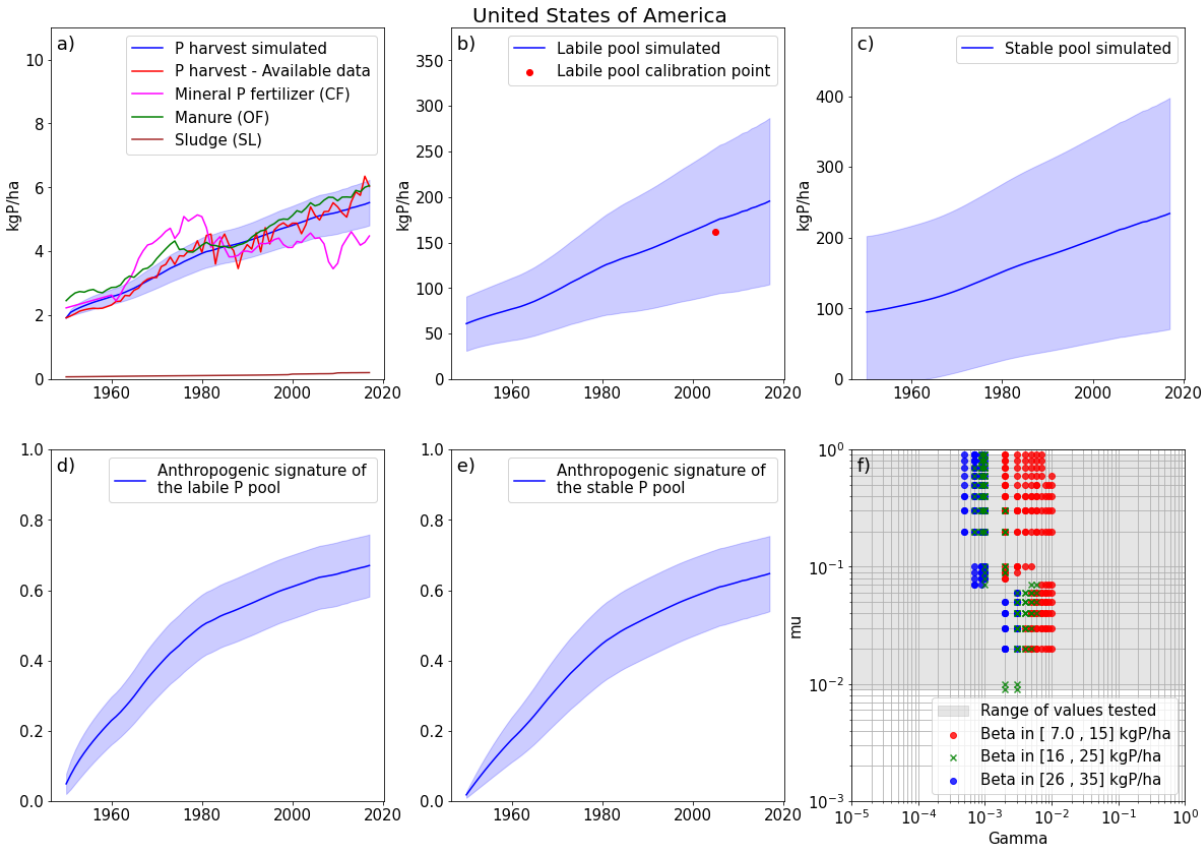


*Figure S23 - Country-specific results: case of the United States of America. From the top to the bottom and from the right to the left: (a) P harvest available information (red) and simulated one, inputs of mineral P fertilizer (pink) and manure (green), (b) Size of the labile pool in kgP.ha$^{-1}$, (c) size of the stable pool in kgP.ha$^{-1}$, (d) anthropogenic signature of the labile pool, (e) anthropogenic signature of the stable pool and (f) values taken by the three calibrated parameters following the calibration procedure. In blue are the simulated values, displayed with a mean value (bold line) and a standard deviation (light blue).*

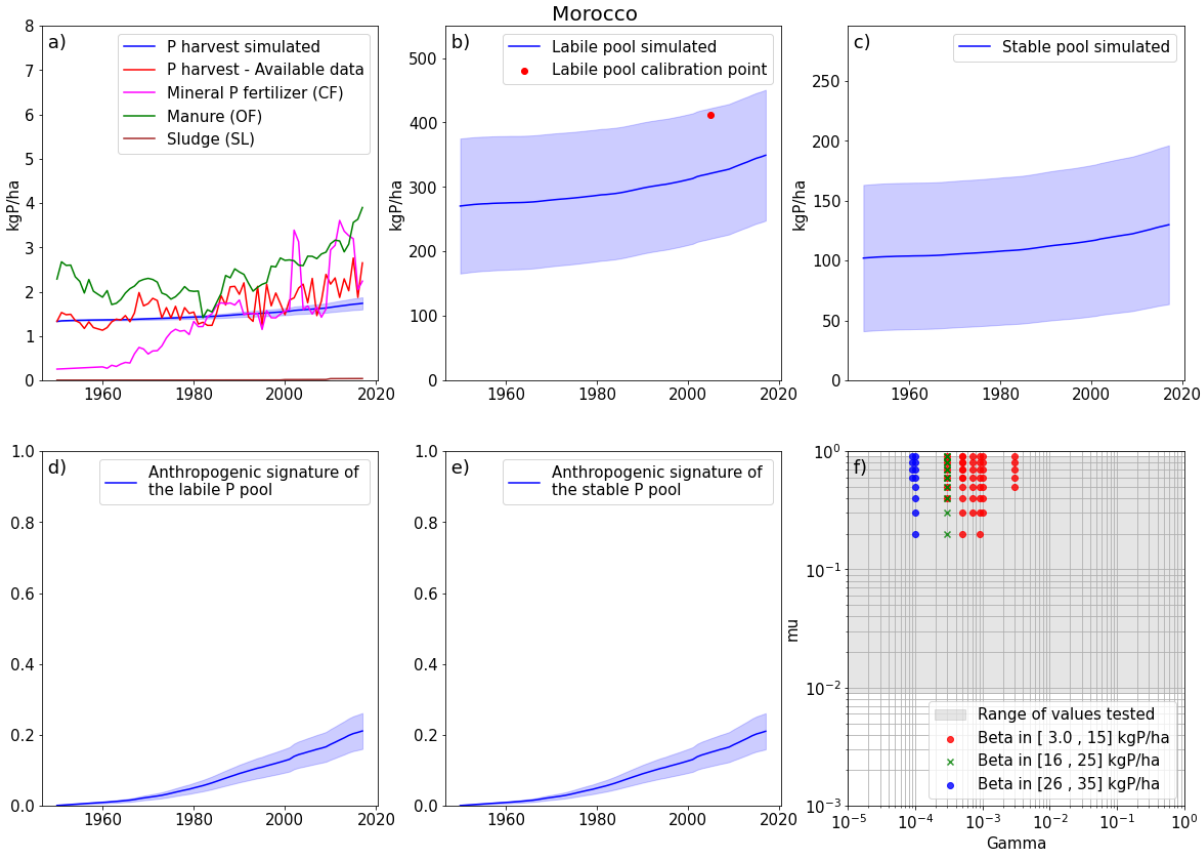


*Figure S24 - Country-specific results: case of Morocco. From the top to the bottom and from the right to the left: (a) P harvest available information (red) and simulated one, inputs of mineral P fertilizer (pink) and manure (green), (b) Size of the labile pool in kgP.ha$^{-1}$, (c) size of the stable pool in kgP.ha$^{-1}$, (d) anthropogenic signature of the labile pool, (e) anthropogenic signature of the stable pool and (f) values taken by the three calibrated parameters following the calibration procedure. In blue are the simulated values, displayed with a mean value (bold line) and a standard deviation (light blue).*

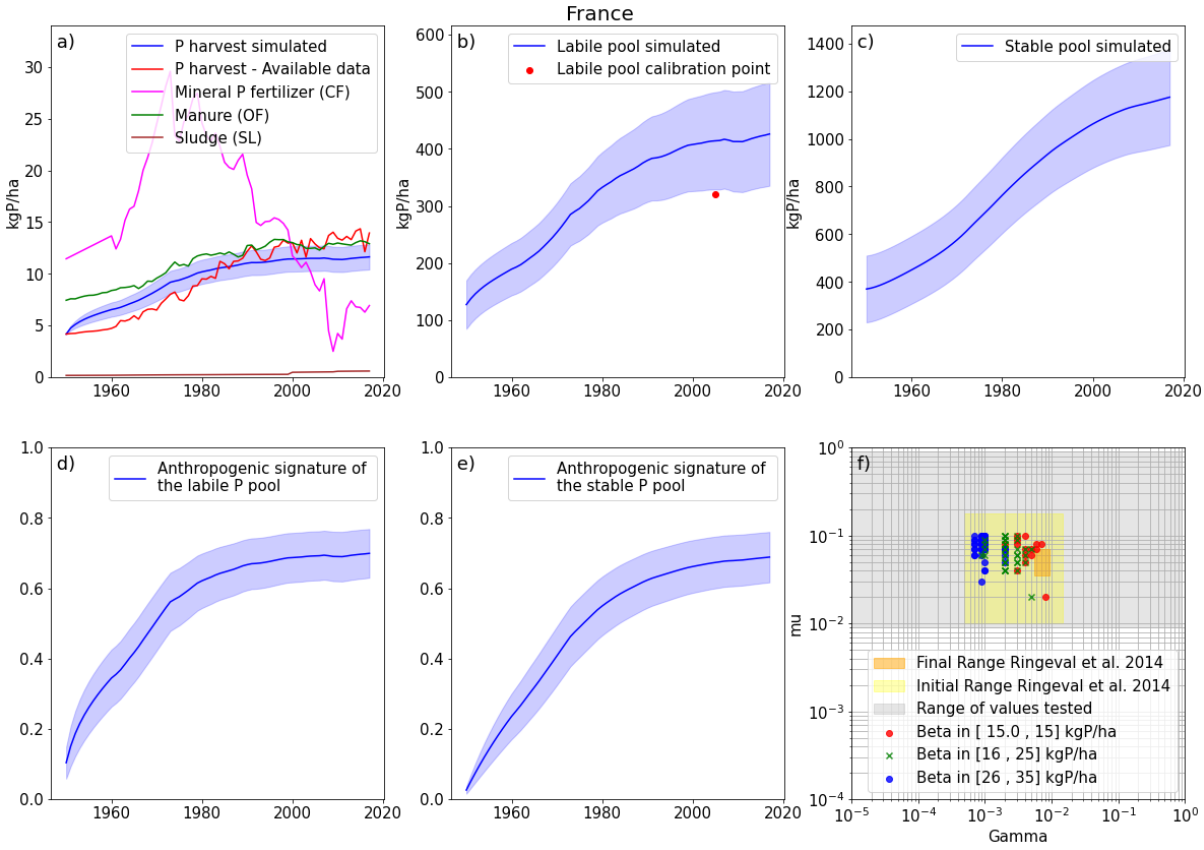


*Figure S25 - Country-specific results: case of France. From the top to the bottom and from the right to the left: (a) P harvest available information (red) and simulated one, inputs of mineral P fertilizer (pink) and manure (green), (b) Size of the labile pool in kgP.ha$^{-1}$, (c) size of the stable pool in kgP.ha$^{-1}$, (d) anthropogenic signature of the labile pool, (e) anthropogenic signature of the stable pool and (f) values taken by the three calibrated parameters following the calibration procedure. In blue are the simulated values, displayed with a mean value (bold line) and a standard deviation (light blue).*

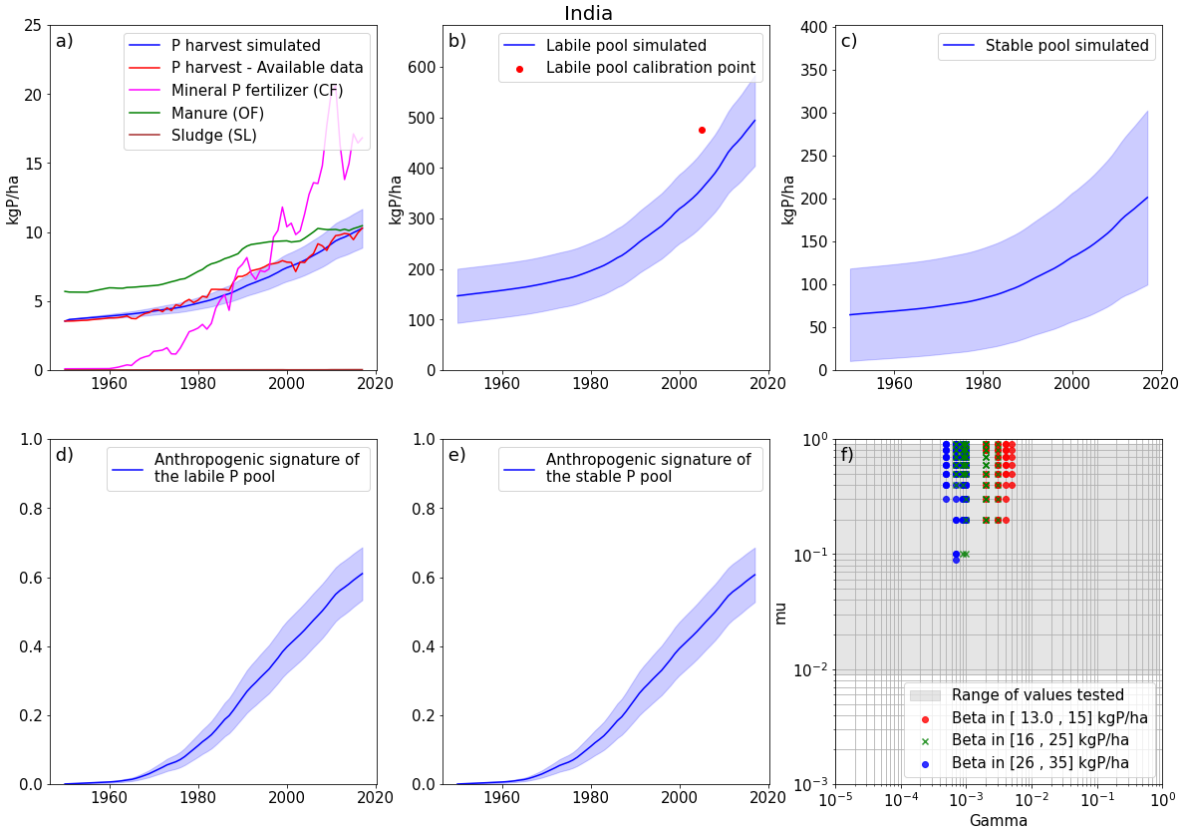


*Figure S26 - Country-specific results: case of India. From the top to the bottom and from the right to the left: (a) P harvest available information (red) and simulated one, inputs of mineral P fertilizer (pink) and manure (green), (b) Size of the labile pool in kgP.ha$^{-1}$, (c) size of the stable pool in kgP.ha$^{-1}$, (d) anthropogenic signature of the labile pool, (e) anthropogenic signature of the stable pool and (f) values taken by the three calibrated parameters following the calibration procedure. In blue are the simulated values, displayed with a mean value (bold line) and a standard deviation (light blue).*

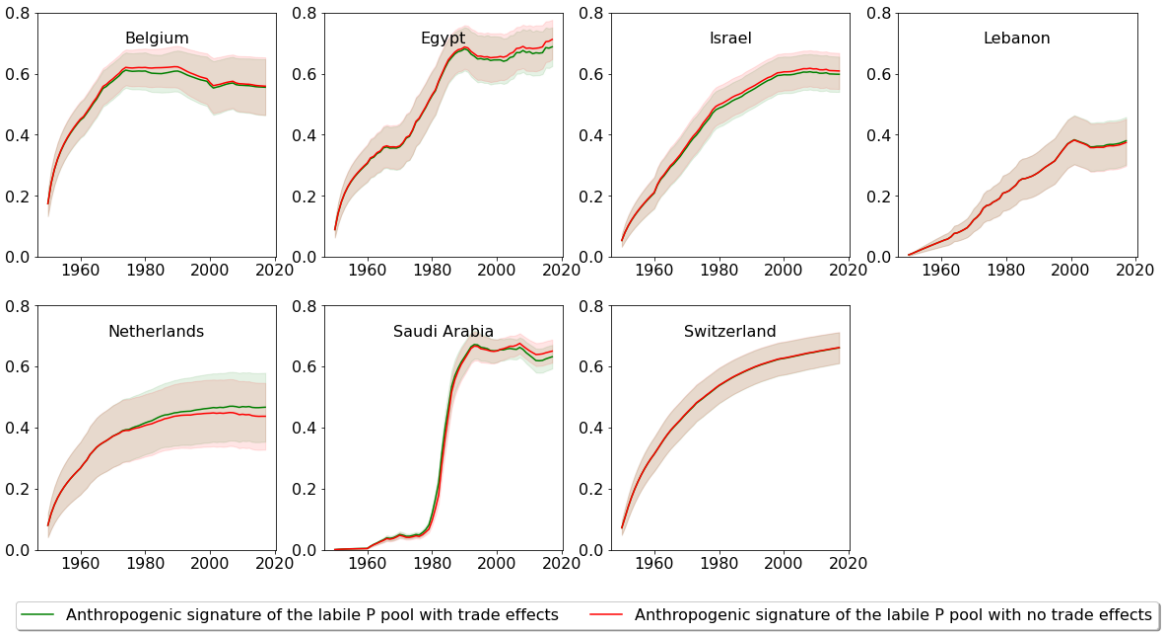


*Figure S27 – Anthropogenic signatures of the soil labile P pool with and without the effect of the trade of agricultural products. In green: results from the main computations. In red: results from computations where we set the anthropogenic signature of all imported food and feed products to that of the importing countries.*

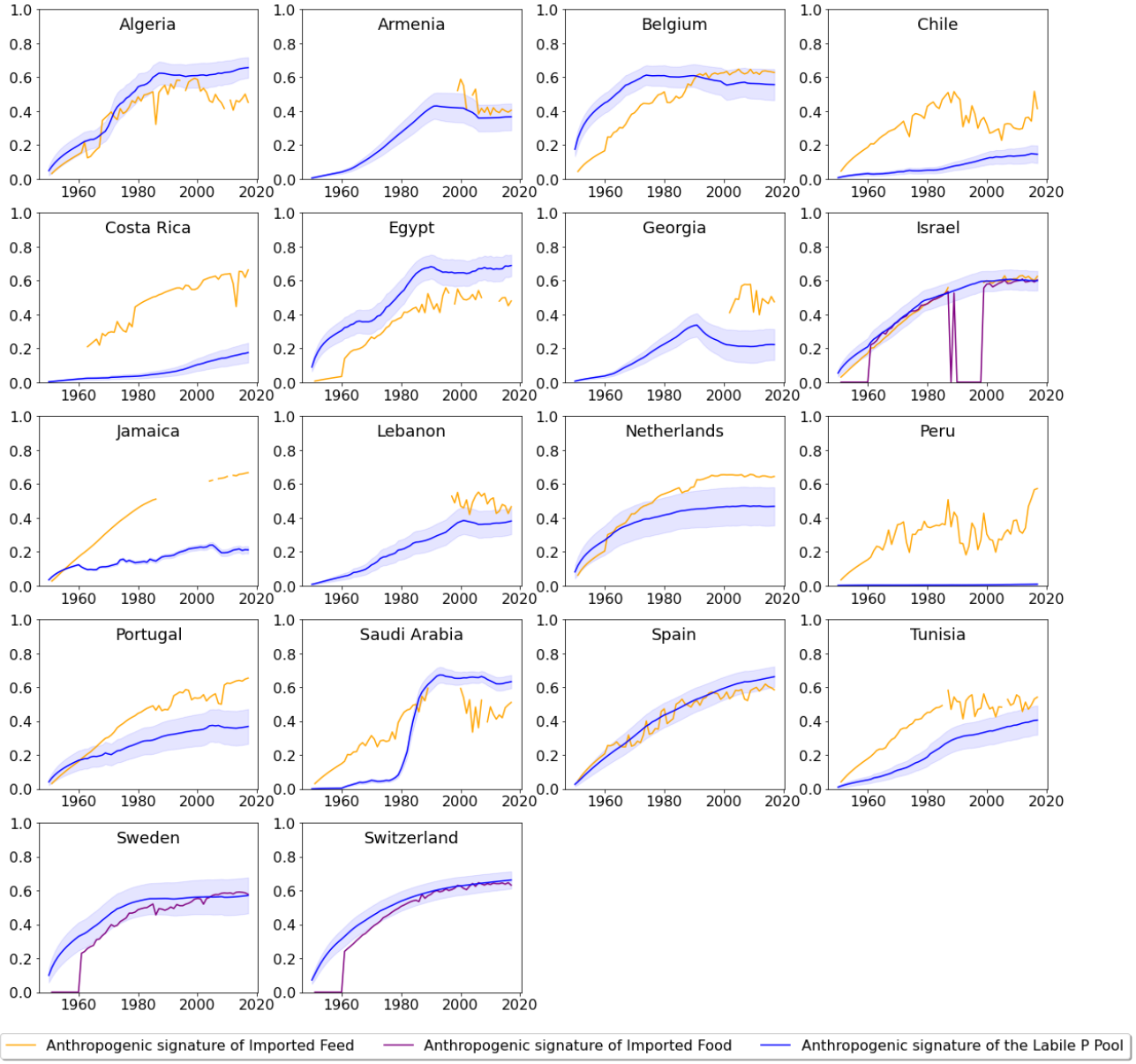


*Figure S28 – Anthropogenic signature of imported feed, food and of the labile pool. Data on the anthropogenic signature of the imported feed were only displayed for the countries in which the contribution soil P inputs coming from imported feed over the 2007-2017 period represented more than 5% of their total cumulative soil P inputs. Data on the anthropogenic signature of the imported food were only displayed for the countries in which the contribution soil P inputs coming from imported food over the 2007-2017 period represented more than 4% of their total cumulative soil P inputs. When no data are displayed in some years this is because the country studied did not import any feed nor food.*

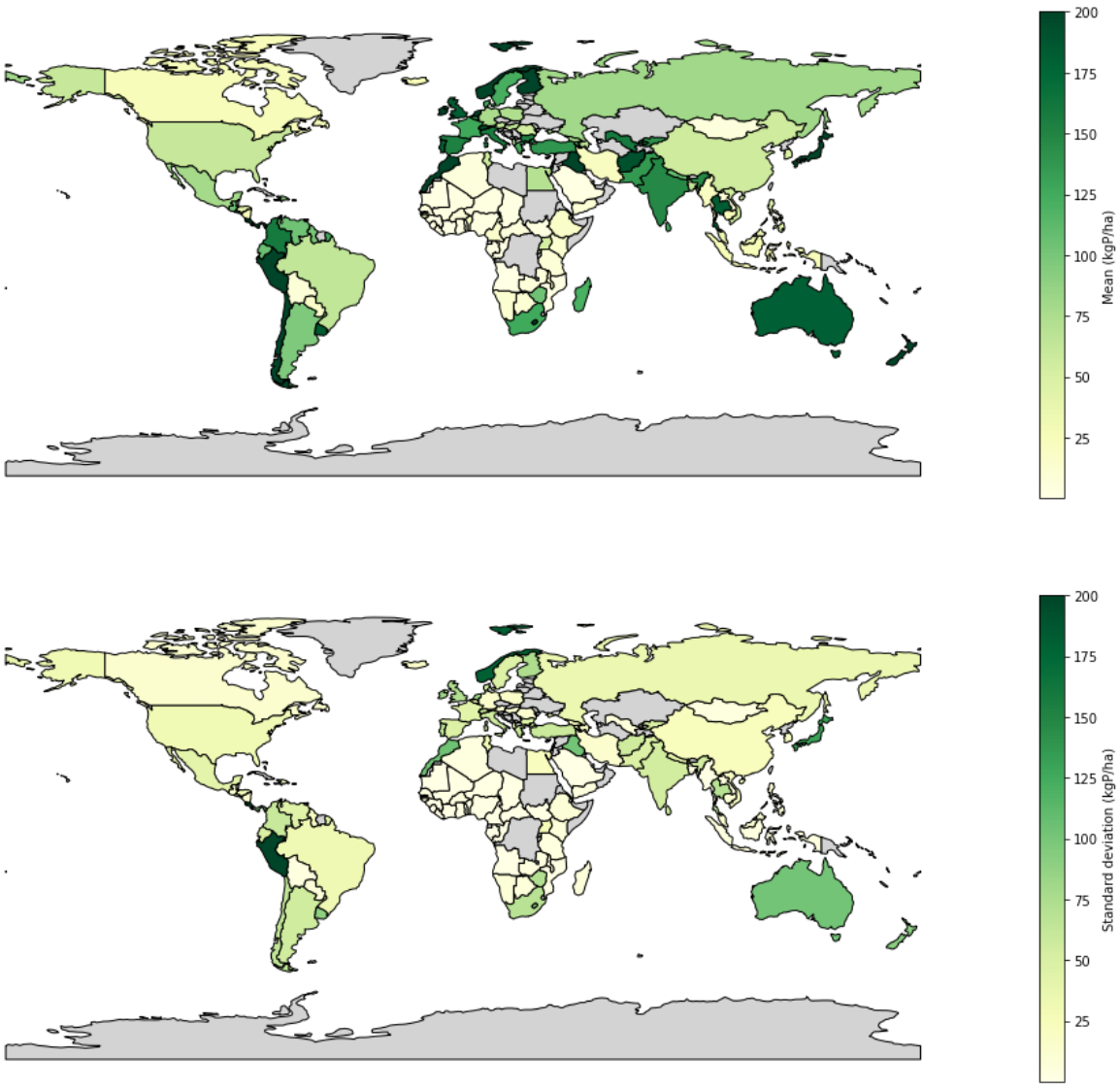


*Figure S29 - Size of the labile P pool of agricultural soils in 1950 for each country: (above) mean value, (below) standard deviation. Data are displayed in kgP.ha$^{-1}$.*

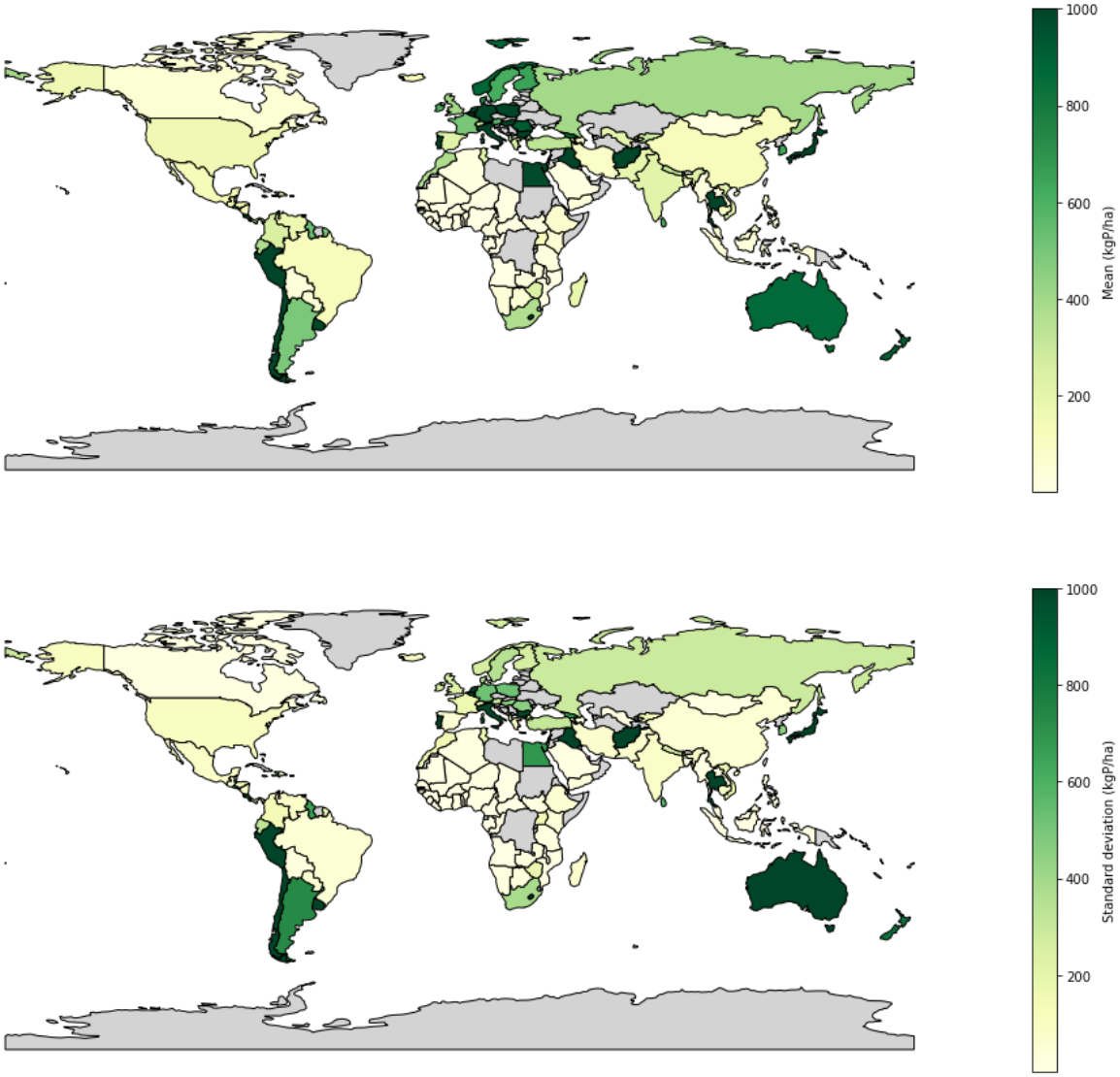


*Figure S30 - Size of the P pools (labile +stable) of agricultural soils in 1950 for each country: (above) mean value, (below) standard deviation. Data are displayed in kgP.ha$^{-1}$*

# Supplementary Tables

*Table S2 - Livestock category considered for the analysis. Some FAOSTAT categories have been grouped into one. Thus, poultry include chickens, ducks, geese, guinea fowls and turkeys. Asses and mules were grouped together, as well as goats and sheep.*

| Main Item | FAOSTAT Item |
|---|---|
| Asses&Mules | Asses |
| | Mules |
| Cattle | Cattle |
| Poultry | Chickens |
| | Ducks |

| | |
|---|---|
| | Geese and guinea fowls |
| | Turkeys |
| Goats&Sheep | Goats |
| | Sheep |
| Horses | Horses |
| Buffaloes | Buffaloes |
| Pigs | Pigs |
| Rabbits and hares | Rabbits and hares |

*Table S3 - P excretion rate data derived from* (Sheldrick et al., 2003)*, except for rabbits and hares. For rabbits and hares, French data were used to calculated a $P_{rate}$, based on slaughtered weight (FAOSTAT) and P excretion* (Ringeval et al., 2014) *data. Data for buffaloes, asses and mules were not provided in Sheldrick et al. For buffaloes we assumed a similar P excretion rate as for cattle. Similarly, for Asses&Mules we assumed the same P excretion rate as for horses.*

| Livestock category | Slaughtered weight (kg) | P excretion (kgP/y/head) | $P_{rate}$ ($kgP.yr^{-1}.kg\ slaughtered\ weight^{-1}$) |
|---|---|---|---|
| Cattle | 250 | 10 | 0.04 |
| Buffaloes | - | - | 0.04 |
| Pigs | 80 | 4 | 0.05 |
| Sheep | 15 | 2 | 0.13 |
| Goats | 12 | 2 | 0.17 |
| Horses | 250 | 8 | 0.03 |
| Asses&Mules | - | - | 0.03 |
| Poultry | 2 | 0.19 | 0.10 |
| Rabbits and hares | 1.46 | 1.09 | 0.75 |

*Table S4 – Energy requirement for each ruminant category considered. Data are derived from* (Barbieri et al., 2021)*.*

| | Energy Requirements ($MJ\ ME.yr^{-1}.kg\ of\ live\ weight^{-1}$) – Req(l) |
|---|---|
| Dairy Cattle | 39 |
| Beef Cows | 72 |
| Sheep Meat | 197 |
| Sheep Milk | 177 |
| Goats Meat | 177 |
| Goats Milk | 180 |

*Table S5 – Items considered for the calculation of cropland P harvest. concP refers to their P concentration derived from (Comifer, 2009).*

| | concP (tP/t DM) |
|---|---|
| **Wheat** | 0.00341 |
| **Maize** | 0.00213 |
| **Rice, Paddy** | 0.00282 |
| **Soybeans** | 0.0055 |
| **Barley** | 0.00342 |
| **Sugar Cane** | 0.00022 |
| **Sorghum** | 0.0033 |
| **Cottonseed** | 0.00524 |
| **Rapeseed** | 0.00546 |
| **Potatoes** | 0.0005 |
| **Sunflower Seed** | 0.00618 |
| **Cotton Lint** | 0.0064 |
| **Oats** | 0.00342 |
| **Onions, Dry** | 0.00243 |
| **Groundnuts, With Shell** | 0.00341 |
| **Vegetables, Fresh Nes** | 0.00052 |
| **Millet** | 0.00275 |
| **Beans, Dry** | 0.00419 |
| **Rye** | 0.00337 |
| **Sweet Potatoes** | 0.00041 |
| **Cassava** | 0.00038 |
| **Sugar Beet** | 0.00022 |
| **Palm Kernels** | 0.0085 |
| **Peas, Dry** | 0.00375 |
| **Coconuts** | 0.00094 |
| **Chick Peas** | 0.00332 |
| **Broad Beans, Horse Beans, Dry** | 0.00426 |
| **Tomatoes** | 0.00022 |
| **Triticale** | 0.0038 |
| **Cocoa, Beans** | 0.00656 |
| **Cabbages And Other Brassicas** | 0.00036 |

*Table S6 – P-Olsen data from the LUCAS topsoil survey* (Jones et al., 2020). *Data are representative of the soil P availability of agricultural soils including croplands and grasslands at year 2015.*

| Country | P mean (mg/kg) | P mean ($kgP.ha^{-1}$) | Number of values above 10mgP/kg | Number of values below 10 mg/kg | P std ($kgP.ha^{-1}$) |
|---|---|---|---|---|---|
| UK | 51.1 | 214.6 | 619 | 6 | 142.9 |
| Slovakia | 34.5 | 145 | 124 | 16 | 84.4 |
| Austria | 36.7 | 154.3 | 265 | 20 | 102.9 |
| Slovenia | 33 | 138.8 | 30 | 12 | 82.2 |
| Finland | 51.5 | 216.4 | 197 | 1 | 107.3 |
| Sweden | 40.4 | 169.6 | 227 | 12 | 113.9 |
| Romania | 26.7 | 112.2 | 431 | 379 | 122.5 |
| Portugal | 31.4 | 132 | 144 | 57 | 103.9 |
| Poland | 50.6 | 212.5 | 934 | 24 | 128.4 |
| Germany | 60.6 | 254.6 | 1216 | 8 | 145.2 |
| Netherlands | 84.1 | 353.2 | 133 | 0 | 136 |
| Latvia | 30.7 | 128.9 | 139 | 13 | 105.6 |
| Luxembourg | 52 | 218.6 | 8 | 0 | 74.3 |
| Lithuania | 27.5 | 115.5 | 206 | 48 | 101.2 |
| Italy | 35.3 | 148.1 | 725 | 328 | 139.6 |
| Ireland | 57.6 | 242 | 157 | 3 | 131.8 |
| Hungary | 31.1 | 130.7 | 267 | 50 | 98.4 |
| Croatia | 44.6 | 187.4 | 16 | 7 | 183.3 |
| France | 41.6 | 174.5 | 2269 | 94 | 119.9 |
| Spain | 32.4 | 135.9 | 1803 | 602 | 124.2 |
| Greece | 32.7 | 137.3 | 228 | 154 | 148.2 |
| Estonia | 34.8 | 146.2 | 83 | 3 | 114.2 |
| Denmark | 49.2 | 206.5 | 182 | 0 | 94.2 |
| Czechia | 45.7 | 191.9 | 309 | 8 | 116.5 |
| Cyprus | 45 | 189.2 | 24 | 9 | 143.6 |
| Bulgaria | 27.6 | 115.9 | 239 | 118 | 95.3 |
| Belgium | 73 | 306.7 | 108 | 0 | 146.8 |
| Malta | 179 | 752 | 2 | 0 | 573.9 |

*Table S7 – Agricultural items considered for trade calculations. P concentration of each product (concP, $tP.tDM^{-1}$) are derived from* (Comifer, 2009). *2 columns are displayed and refer respectively to the P concentration of aggregated items from the Food Balances database and to the P concentration of more detailed items described in the Detailed Trade Matrix database. "Delta Feed" was used to differentiate between commodities that were consumed as feed only (1), food only (0) or as both.*

*In this last case, the fractions of imported quantities used for feed and food were country-specific and computed with Equation **S26** and Equation **S28**.*

| Items Aggregated | As referred to in Food Balances | concP (tP/t DM) | As referred to in Detailed Trade Matrix | Delta Feed | concP (tP/t DM) |
|---|---|---|---|---|---|
| **Maize** | Maize and products | 0.00213 | Bran, maize | 1 | 0.01143 |
| | | | Cake, maize | 1 | 0.0091 |
| | | | Maize | Eq. S26-S28 | 0.00213 |
| | | | Maize, green | 1 | 0.00083 |
| | | | Feed and meal, gluten | 1 | 0.0019 |
| **Soybeans** | Soyabeans | 0.0055 | Cake, soybeans | 1 | 0.0071 |
| | | | Soybeans | Eq. S26-S28 | 0.0055 |
| **Wheat** | Wheat and products | 0.00341 | Bran, wheat | 1 | 0.01143 |
| | | | Flour, wheat | 0 | 0.00175 |
| | | | Wheat | Eq. S26-S28 | 0.00341 |
| | | | Pastry | 0 | 0.00153 |
| | | | Grain, mixed | 1 | 0.00341 |
| **Rape And Mustardseed** | Rape and Mustardseed | 0.00546 | Cake, rapeseed | 1 | 0.0129 |
| | | | Rapeseed | Eq. S26-S28 | 0.00546 |
| **Barley** | Barley and products | 0.00342 | Barley | Eq. S26-S28 | 0.00342 |
| **Rice** | Rice and products | 0.00282 | Rice, paddy (rice milled equivalent) | Eq. S26-S28 | 0.00282 |
| | | | Rice, milled | Eq. S26-S28 | 0.00114 |
| **Sunflower** | Sunflower seed | 0.00618 | Cake, sunflower | 1 | 0.0113 |
| | | | Sunflower seed | Eq. S26-S28 | 0.00618 |
| **Palm Kernel** | Palm kernels | 0.0085 | Cake, palm kernel | 1 | 0.0085 |
| **Milk** | Milk - Excluding Butter | 0.00580 | Cheese, whole cow milk | 0 | 0.005 |
| | | | Milk, skimmed dried | Eq. S26-S28 | 0.0102 |
| | | | Milk, whole dried | Eq. S26-S28 | 0.00714 |
| | | | Milk, whole fresh cow | Eq. S26-S28 | 0.00092 |
| | | | Whey, dry | 1 | 0.00576 |
| **Sorghum** | Sorghum and products | 0.0033 | Sorghum | Eq. S26-S28 | 0.0033 |
| **Cocoa** | Cocoa Beans and products | 0.00451 | Cocoa, beans | 0 | 0.00656 |
| | | | Cocoa, powder & cake | 0 | 0.00656 |
| | | | Cocoa, paste | 0 | 0.00656 |
| | | | Cocoa, butter | 0 | 0 |

| | | | | | |
|---|---|---|---|---|---|
| | | | Chocolate products nes | 0 | 0.00287 |
| **Meat, Chicken** | Poultry Meat | 0.00165 | Meat, chicken | 0 | 0.00165 |
| **Peas** | Peas | 0.00375 | Peas, dry | Eq. S26-S28 | 0.00375 |
| **Onions** | Onions | 0.00243 | Onions, dry | 0 | 0.00243 |
| **Beans** | Beans | 0.00419 | Beans, dry | Eq. S26-S28 | 0.00419 |
| **Coffee** | Coffee and products | 0.00181 | Coffee, green | 0 | 0.0016 |
| | | | Coffee, roasted | 0 | 0.00192 |
| | | | Coffee, extracts | 0 | 0.00192 |
| **Bovine Meat** | Bovine Meat | 0.0019 | Meat, cattle, boneless (beef & veal) | 0 | 0.0019 |
| **Meat, Pig** | Pigmeat | 0.00192 | Meat, pig | 0 | 0.00192 |
| | | | Meat, pork | 0 | 0.00192 |
| **Oats** | Oats | 0.00342 | Oats | Eq. S26-S28 | 0.00342 |
| | | | Oats rolled | Eq. S26-S28 | 0.00415 |
| **Sugar** | Sugar cane | 0.00017 | Sugar crops nes | 0 | 0.00024 |
| | Sugar beet | 0.00022 | Sugar beet | 0 | 0.00022 |
| | Sugar (Raw Equivalent) | 0.00024 | Sugar Raw Centrifugal | 0 | 0.00024 |
| | Sugar non-centrifugal | 0 | Sugar non-centrifugal | 0 | 0 |
| **Millet** | Millet and products | 0.00709 | Bran, millet | 1 | 0.01143 |
| | | | Millet | Eq. S26-S28 | 0.00275 |
| **Rye** | Rye and products | 0.00337 | Rye | Eq. S26-S28 | 0.00337 |
| **Sweet Potatoes** | Sweet potatoes | 0 | Sweet potatoes | 0 | 0.00041 |
| **Potatoes** | Potatoes and products | 0.0005 | Flour, potatoes | Eq. S26-S28 | 0.0005 |
| | | | Potatoes | Eq. S26-S28 | 0.0005 |
| | | | Potatoes, frozen | Eq. S26-S28 | 0.0005 |
| **Bananas** | Bananas | 0.00023 | Bananas | 0 | 0.00023 |

*Table S8 - Cumulated use of mineral P fertilizer over the 1950-2017 period, for each large world region.*

| World Region | Mean cumulated application of mineral P fertilizer over the 1950-2017 period ($kgP.ha^{-1}$) |
|---|---|
| Asia | 249 |
| Western Europe | 777 |
| Africa | 25 |
| South and Central America | 112 |
| Eastern Europe | 215 |

| | |
|---|---|
| Oceania | 76 |
| Northern America | 261 |

## References


Barbieri, P., Pellerin, S., Seufert, V., Smith, L., Ramankutty, N., Nesme, T., 2021. The global option space for organic agriculture under nitrogen limitations. Nat. Food 2, 363–372. https://doi.org/https://dx.doi.org/10.1038/s43016-021-00276-y

Batjes, N.H., 2010. Inventory of P-Olsen data in the ISRIC-WISE soil database for use with QUEFTS: (version 1.0)., Report - ISRIC World Soil Information.

Comifer, 2009. Teneur en P, K et Mg des organes végétaux récoltés. COMIFER.

Cordell, D., White, S., 2014. Life's bottleneck: Sustaining the world's phosphorus for a food secure future. Annu. Rev. Environ. Resour. 39, 161–188. https://doi.org/10.1146/annurev-environ-010213-113300

Hengl, T., Leenaars, J.G.B., Shepherd, K.D., Walsh, M.G., Heuvelink, G.B.M., Mamo, T., Tilahun, H., Berkhout, E., Cooper, M., Fegraus, E., Wheeler, I., Kwabena, N.A., 2017. Soil nutrient maps of Sub-Saharan Africa: assessment of soil nutrient content at 250 m spatial resolution using machine learning. Nutr. Cycl. Agroecosystems 109, 77–102. https://doi.org/10.1007/s10705-017-9870-x

Herrero, M., Havlík, P., Valin, H., Notenbaert, A., Rufino, M.C., Thornton, P.K., Blümmel, M., Weiss, F., Grace, D., Obersteiner, M., 2013. Biomass use, production, feed efficiencies, and greenhouse gas emissions from global livestock systems. Proc. Natl. Acad. Sci. U. S. A. 110, 20888–20893. https://doi.org/10.1073/pnas.1308149110

IPNI, 2015. Soil Test Levels In North America. Summary Update: International Plant Nutrition Institute (IPNI).

Jones, A., Fernandez-Ugalde, O., Scarpa, S., 2020. LUCAS 2015 Topsoil Survey. Presentation of dataset and results. Luxembourg. https://doi.org/10.2760/616084

Klein Goldewijk, K., Beusen, A., Doelman, J., Stehfest, E., 2017. Anthropogenic land use estimates for the Holocene – HYDE 3.2. Earth Syst. Sci. Data 9. https://doi.org/https://doi.org/10.5194/essd-9-927-2017

Le Noë, J., Roux, N., Gingrich, S., Erb, K.-H., Krausmann, F., Thieu, V., Silvestre, M., Garnier, J., 2020. The phosphorus legacy offers opportunities for agro-ecological transition (France 1850–2075). Environ. Res. Lett. 15. https://doi.org/10.1088/1748-9326/ab82cc

Lu, C., Tian, H., 2016. Global nitrogen and phosphorus fertilizer use for agriculture production in the past half century: shifted hot spots and nutrient imbalance. Earth Syst. Sci. Data 9, 181–192. https://doi.org/https://doi.org/10.5194/essd-9-181-2017

Mitchell, B.R., 1998a. International Historical Statistics: Europe 1750 -1993.

Mitchell, B.R., 1998b. International Historical Statistics-Africa, Asia and Oceania 1750-1993.

Mitchell, B.R., 1993. International Historical Statistics - The Americas.

Ringeval, B., Augusto, L., Monod, H., Van Apeldoorn, D., Bouwman, L., Yang, X., Achat, D.L., Chini, L.P., Van Oost, K., Guenet, B., Wang, R., Decharme, B., Nesme, T., Pellerin, S., 2017. Phosphorus in agricultural soils: drivers of its distribution at the global scale. Glob. Chang. Biol. 23, 3418–

3432. https://doi.org/10.1111/gcb.13618

Ringeval, B., Nowak, B., Nesme, T., Delmas, M., Pellerin, S., 2014. Contribution of anthropogenic phosphorus to agricultural soil fertility and food production. Global Biogeochem. Cycles 28, 743–756. https://doi.org/10.1002/ 2014GB004842

Sattari, S.Z., Bouwman, A.F., Giller, K.E., Van Ittersum, M.K., 2012. Residual soil phosphorus as the missing piece in the global phosphorus crisis puzzle. Proc. Natl. Acad. Sci. U. S. A. 109, 6348–6353. https://doi.org/10.1073/pnas.1113675109

Sheldrick, W., Keith Syers, J., Lingard, J., 2003. Contribution of livestock excreta to nutrient balances. Nutr. Cycl. Agroecosystems 66, 119–131. https://doi.org/10.1023/A:1023944131188

Smil, V., 2000. Phosphorus in the Environment: Natural Flows and Human Interferences. Annu. Rev. Energy Environ. 25, 53–88. https://doi.org/https://doi.org/10.1146/annurev.energy.25.1.53

Van Oost, K., Quine, T.A., Govers, G., De Gryze, S., Six, J., Harden, J.W., Ritchie, J.C., McCarty, G.W., Heckrath, G., Kosmas, C., Giraldez, J. V., Marques Da Silva, J.R., Merckx, R., 2007. The Impact of Agricultural Soil Erosion on the Global Carbon Cycle. Science (80-. ). 318, 626–629. https://doi.org/10.1126/science.1145724

Van Puijenbroek, P., Beusen, A.H.W., Bouwman, A.F., 2019. Global nitrogen and phosphorus in urban waste water based on the Shared Socio-economic pathways. J. Environ. Manage. 231, 446–456. https://doi.org/10.1016/j.jenvman.2018.10.048

Yang, X., Post, W.M., Thornton, P.E., Jain, A., 2013. The distribution of soil phosphorus for global biogeochemical modeling. Biogeosciences 10, 2525–2537. https://doi.org/10.5194/bg-10-2525-2013

Zhang, J., Beusen, A., van Apeldoorn, D., Mogollón, J., Yu, C., Bouwman, A., 2017. Spatiotemporal dynamics of soil phosphorus and crop uptake in global cropland during the twentieth century. Biogeosciences 14, 2055–2068. https://doi.org/10.5194/bg-2016-543